AGU PUBLICATIONS

Water Resources Research

RESEARCH ARTICLE
10.1002/2017WR020854

Key Points:
- Persistent, abundant invaders out-compete native species and increase hydro-morphodynamic pressures at colonization sites
- Less persistent invaders facilitate native vegetation by decreasing hydro-morphodynamic pressures at colonization sites
- Seasonal, dynamic properties of invaders and native species determine hydro-morphodynamic invasion effects

Supporting Information:
- Supporting Information S1
- Movie S1
- Movie S2
- Movie S3

Correspondence to:
M. van Oorschot,
mijke.vanoorschot@deltares.nl

Citation:
van Oorschot, M., M. G. Kleinhans, G. W. Geerling, G. Egger, R. S. E. W. Leuven, and H. Middelkoop (2017), Modeling invasive alien plant species in river systems: Interaction with native ecosystem engineers and effects on hydro-morphodynamic processes, *Water Resour. Res.*, *53*, 6945–6969, doi:10.1002/2017WR020854.

Received 3 APR 2017
Accepted 16 JUL 2017
Accepted article online 20 JUL 2017
Published online 17 AUG 2017

Modeling invasive alien plant species in river systems: Interaction with native ecosystem engineers and effects on hydro-morphodynamic processes

M. van Oorschot[1,2], M. G. Kleinhans[1], G. W. Geerling[2,3], G. Egger[4], R. S. E. W. Leuven[5,6], and H. Middelkoop[1]

[1]Faculty of Geosciences, Utrecht University, TC Utrecht, The Netherlands, [2]Deltares, Department of Freshwater Ecology and Water Quality, Delft, The Netherlands, [3]Institute for Science Innovation and Society, Radboud University, Nijmegen, The Netherlands, [4]Institute of Floodplain Ecology, Karlsruhe Institute of Technology, Rastatt, Germany, [5]Department of Environmental Science, Institute for Water and Wetland Research, Radboud University, Nijmegen, The Netherlands, [6]Netherlands Centre of Expertise for Exotic Species, Nijmegen, The Netherlands

Abstract Invasive alien plant species negatively impact native plant communities by out-competing species or changing abiotic and biotic conditions in their introduced range. River systems are especially vulnerable to biological invasions, because waterways can function as invasion corridors. Understanding interactions of invasive and native species and their combined effects on river dynamics is essential for developing cost-effective management strategies. However, numerical models for simulating long-term effects of these processes are lacking. This paper investigates how an invasive alien plant species affects native riparian vegetation and hydro-morphodynamics. A morphodynamic model has been coupled to a dynamic vegetation model that predicts establishment, growth and mortality of riparian trees. We introduced an invasive alien species with life-history traits based on Japanese Knotweed (*Fallopia japonica*), and investigated effects of low- and high propagule pressure on invasion speed, native vegetation and hydro-morphodynamic processes. Results show that high propagule pressure leads to a decline in native species cover due to competition and the creation of unfavorable native colonization sites. With low propagule pressure the invader facilitates native seedling survival by creating favorable hydro-morphodynamic conditions at colonization sites. With high invader abundance, water levels are raised and sediment transport is reduced during the growing season. In winter, when the above-ground invader biomass is gone, results are reversed and the floodplain is more prone to erosion. Invasion effects thus depend on seasonal above- and below ground dynamic vegetation properties and persistence of the invader, on the characteristics of native species it replaces, and the combined interactions with hydro-morphodynamics.

1. Introduction

Alien plant species that become dominant in their introduced range can have disastrous effects on functioning of ecosystems by out-competing native species and changing abiotic and biotic conditions in their new environment, subsequently restructuring native plant communities and threatening biodiversity [*Richardson et al.*, 2007; *Santoro et al.*, 2012]. Propagules of potential invasive plants can be transported as "hitchhikers" attached to car tires, in ballast water of ships, or may originate from escapes or soil deposits of gardens, where they were introduced as ornamental plants [*Simberloff*, 2013]. Riparian zones are especially susceptible to alien species because waterways function as invasion corridors and are efficient transport vectors for plant propagules [*Grime*, 2001; *Horvitz et al.*, 2014].

River regulation can promote invasion success, when the altered hydro-morphological conditions favor plant species that disperse more rapidly or are better adapted to the new conditions than native species [*Perkins et al.*, 2015]. Invasive species are able to rapidly change their phenology by elongating their roots and thereby gain competitive advantage over natives [*Stromberg et al.*, 2007a; *Flanagan et al.*, 2015]. Groundwater dynamics strongly influences biogeomorphic succession of riparian vegetation, especially in situations where access to groundwater is more limiting [*Batz et al.*, 2016]. Flow regime alterations can therefore induce a dominance shift from native to invasive species [*Stromberg et al.*, 2007b], while it is more difficult for the invader to become dominant in natural systems [*Merritt and Poff*, 2010].

An invasive plant species that is currently causing severe ecological and economical damage in Europe is Japanese Knotweed (*Fallopia japonica*) [*Shaw et al*., 2011; *Stoll et al*., 2012]. This is a perennial herb that forms impenetrable dense patches with stems up to 3 m high, combined with an extensive, below-ground rhizome network [*Weston et al*., 2005]. It is adapted to highly disturbed habitats, allowing it to persist in a wide range of environmental conditions. *F. japonica* originates from Japan where it occurs in mountainous areas, and it has been imported in north-western Europe for ornamental purposes [*Shimoda and Yamasaki*, 2016]. To date, this species is rapidly spreading across riparian systems by clonal growth or (re)sprouting from rhizome parts that are deposited on river bars and banks [*Beerling et al*., 1994].

F. japonica can become dominant because it occupies similar recruitment sites as native riparian species [*Gerber et al*., 2008], while it is a strong competitor due to its rapid growth and ability to produce allelopathic substances that reduce grazing and establishment of other plant species [*Beerling et al*., 1994; *Dommanget et al*., 2014]. A lack of new recruitment sites for riparian trees combined with densely vegetated *F. japonica* patches will prevent rejuvenation as well as natural succession toward the climax phase of native riparian vegetation [*Aguilera et al*., 2010]. Because all *F. japonica* plants in Europe are genetically similar, they are assumed to be clones from one plant, and therefore vegetative dispersal has been the dominant mode of reproduction [*Groeneveld et al*., 2014]. However, it is known that *F. japonica* can be fertilized by Giant Knotweed (*Fallopia sachalinensis*), creating a hybrid called Bohemian Knotweed (*Fallopia x bohemica*). This hybrid has similar characteristics as *F. japonica*, some even more vigorous, but it is also able to reproduce via seeds. These seeds are buoyant, while water increases their germination rate [*Gillies et al*., 2016]. This means that the distribution of *Fallopia* hybrids toward downstream areas can expand even more rapidly in riparian areas. Because of its high invasive potential *F. japonica* is listed as one of the 100 most invasive species by the International Union for Conservation of Nature (IUCN) [*Lowe et al*., 2000].

Several case studies showed that riparian plant invaders change the native vegetation composition through outcompeting native plants and by creating dense mono-stands [*Child and Wade*, 2000]. This, in turn, affects river hydrodynamics and bio-geomorphodynamics by changing sedimentation and erosion processes: for instance, the establishment of persistent dense stands of *Tamarix* on river banks in America and Australia increased hydraulic resistance and sediment trapping of the floodplain, thereby narrowing the river channel and stabilizing the floodplain [*Tickner et al*., 2001]. Another example is the impact of alien Willow species *(Salix spp.)* in Australia and New-Zealand, initially planted to prevent erosion, but have become invasive and are now negatively affecting stream ecosystems [*Doody et al*., 2011]. Contrastingly, there are also invasive plants of which the above-ground biomass dies in winter, such as *F. japonica* and *Impatiens glandulifera*, exposing substrate which is more prone to erosion during winter floods [*Beerling and Perrins*, 1993; *Greenwood and Kuhn*, 2014]. As plant structure, thickness, height, and density, influence the hydromorphodynamics of riparian areas [*Gurnell*, 2014; *Batz et al*., 2016; *van Oorschot et al*., 2016], these traits and the life history strategy of the invader as well as the native species they replace, also determine the long-term change in river morphology. Furthermore, effects of invasive species do not necessarily have to be negative for native species when conditions are altered to create new suitable niches. This facilitation is a well-known process for native eco-engineering species. For instance, established pioneer riparian trees trap sediment and thereby enhance seed deposition and facilitate colonization of other plants [*Corenblit et al*., 2016]. This process can also be driven by alien species that actively modify their environment by creating suitable niches for other native species, e.g., organisms creating biotic substrate which supports a higher macro-invertebrate diversity in lakes and estuarine environments [*Bially and MacIsaac*, 2000; *Castilla et al*., 2004] or alien sea-grass *Zostera japonica* promoting faunal diversity [*Posey*, 1988]. However, habitat modification by invasive species can be negative for other native species and can lead to shifts in trophic pathways and potentially alter biodiversity [*Rodriguez*, 2006].

Many models exist for predicting invasive species, their behavior and effects in their introduced ranges. Studies using these models have generated understanding on where suitable habitats are for invasive species [*Peterson and Vieglais*, 2001], how fast they spread [*Hastings et al*., 2004], how native communities are influenced [*Thomson*, 2005; *Eppinga et al*., 2011; *Xiao et al*., 2012; *Allstadt et al*., 2012], what the potential ecosystem effects are and how these can be mitigated [*Buckley et al*., 2003]. However, most of these studies used small-scale or conceptual models with a short time horizon [*Solari et al*., 2016], while the interactions between invasive species, native vegetation and river hydro-morphodynamics involve processes with times scales of decades to centuries that act not only locally but at the landscape scale through interaction with

backwater effects and bar-forming processes [*Habersack*, 2000]. Hence, these interactions between invasive alien species and landforms remain to be studied at this land-forming timescale [*Fei et al*., 2014]. Understanding plant invasions and their interaction with hydro-morphodynamic processes in rivers is crucial for predicting how river systems are affected by invasive alien species, and for prevention or mitigating their negative effects [*Tickner et al*., 2001]. This information is needed to assess risks of establishment, (secondary) spread and impacts of invasive alien species [*EC*, 2014], but we currently lack adequate forecasting models [*Fei et al*., 2014]. Therefore, there is a need to develop models that include interactions between invasive and native species and river morphodynamics at larger spatial and temporal scales.

The aim of this study is to gain understanding of the long-term effects of invasive plant species on native vegetation cover and river hydro-morphodynamics. To this end, we used the Delft3D process-based morphodynamic model coupled to an improved version of the dynamic vegetation model of *van Oorschot et al*. [2016]. By combination of these models we are, for the first time, able to simulate dynamic interactions between native and invasive vegetation and river hydro-morphodynamics over several decades. We included an invasive species with traits and a life-history strategy based on *F. japonica* and modeled its invasion in a meandering river reach. We explored the effects on native riparian vegetation cover, interaction with hydro-morphodynamic processes and long-term morphological development for two scenarios with different dispersal mechanisms of the invasive species, i.e., vegetative dispersal representing low propagule pressure and vegetative dispersal combined with seed dispersal representing high propagule pressure. Additionally, several scenarios with various levels of invader persistence and seeding density were run. All invader scenarios were compared to a reference situation without invaders.

2. Invasion of *Fallopia japonica* in European Rivers

F. japonica is recorded on many floodplains in Western Europe. To illustrate the diversity of river systems and floodplains invaded by *F. japonica*, we give an overview of the invasion behavior and a

Figure 1. Aerial photos of three different rivers with riparian areas invaded by *F. japonica*. Source: Google Earth, accessed July 2016.

Table 1. General Morphodynamic Characteristics of the Case Study Rivers

Characteristic	Unit	Saar[a]	Schwechat[b]	Allier[c]
Coordinates	[°N,°E]	[49°18′59.89, 6°46′22.76]	[47°59′57.39, 16°16′52.41]	[46°30′21.50, 3°19′53.33]
Channel width	*m*	55	10	50
Slope	m/km	0.6	5.2	0.83
Sinuosity		1.28	1.42	1.39
Sediment type		Sand	Gravel	Gravel
D50	*m*	NA	0.03	0.005
Channel forming discharge[d]	m^3/s	NA	53 (bf)	500 (m_{afd})
Level of regulation		High	Low	Low
Mean relative area increase *F. japonica*	%/yr	15	0.33	NA

[a]Data from Google Earth, *Vollmer* [2012] and German waterways and shipping administration.
[b]Data from *Gruener* [2016].
[c]Data from *Van Dijk et al.* [2014] and *Geerling et al.* [2006].
[d]bf = bankfull discharge, m_{afd} = mean annual flood discharge.

morphodynamic description in affected reaches of three rivers that differ in size, morphodynamic activity and regulation level: the Saar River in Germany, the Schwechat River in Austria and the Allier River in France (Figure 1 and Table 1). The Saar River is a heavily modified, intermediate sized river with fixed banks and a static floodplain, making it a representative for many modified floodplains where most floods do not leave the main channel. The river reach in the Schwechat near Traiskirchen is a small, free flowing, meandering stretch [*Gruener*, 2016]. The reach in the Allier River is a highly dynamic medium-sized meandering gravel bed reach in central France, characterized by semi-natural riparian vegetation of which morphodynamics and vegetation have been well documented in the past decades [e.g., *Geerling et al.*, 2006; *Kleinhans and van den Berg*, 2011; *Van Dijk et al.*, 2014]. When these rivers are morphologically compared to a range of other rivers, described in *Kleinhans and van den Berg* [2011], we see that the Saar is comparable to most sandy, lowland rivers, but with intense regulation, so there is no lateral movement of the channel. The Schwechat is a coarse-gravel bed river with a high threshold for movement and the Allier falls between the sand- and gravel-bed rivers with its sandy gravel sediment and naturally eroding banks.

A three-year field study on the floodplains of the Saar River in the area between Saarbrücken and Saarlouis showed a rapid expansion of *F. japonica*, with a relative mean annual area expansion of over 15% [*Vollmer*, 2012]. In the Schwechat the mean annual area expansion of *F. japonica* is calculated at 0.3% from aerial photos from 1971 to 2015 [*Gruener*, 2016]. The development in spatial extension of *F. japonica* mapped from these aerial photos (Figure 2, adapted from *Gruener* [2016]) shows that *F. japonica* expands in all directions around the oldest mapped stand.

As for many rivers, there is no data available yet on *F. japonica* expansion along the Allier River. However, field observations show massive expansion of *F. japonica* seedlings on bare gravel bars in some areas (observations by GE in the Allier). Preliminary studies on the dispersal mechanisms of *F. japonica* in both the Schwechat and the Allier shows that dispersal via rhizomes in sediment combined with lateral expansion are the dominant dispersal processes (observations by GE in the Allier and Schwechat rivers). This concise overview shows that *F. japonica* is able to invade different types of rivers with varying invasion speed.

3. Methods

We are interested in the continuous interaction between vegetation and morphodynamics, as opposed to systems dominated by either vegetation or morphodynamics. Morphodynamics are defined here as the dynamic processes of water flow, sediment transport and depositional processes on the floodplain, resulting in channel migration and together shape river morphology. The Allier River described in section 2 was selected as the inspiration for our idealized modeling study. This river was chosen because it is a medium sized, natural meandering river where vegetation and morphodynamics regularly interact. Moreover, the morphodynamics and vegetation have been well documented over the last years [*Geerling et al.*, 2006;

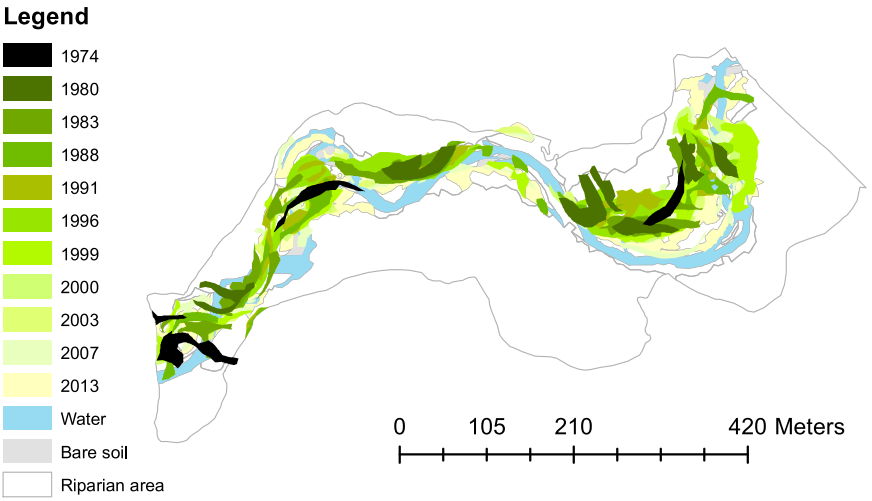

Figure 2. Mapped areal cover of *F. japonica* in the Schwechat river for several years based on aerial imagery from the study of *Gruener* [2016]. Water, bare soil and the riparian area boundaries are derived from the 2013 map.

Kleinhans and van den Berg, 2011; *Van Dijk et al*., 2014], which provided data to calibrate the model and verify model behaviour.

3.1. Model Scenarios

We ran three main scenarios: (1) a reference scenario without invaders, including only Salicaceae, of which the colonization and growth characteristics were calibrated by adjusting the mortality thresholds for flooding, desiccation and uprooting to approximate the vegetation cover and age distribution along the Allier River [*Geerling et al*., 2006]; (2) a scenario where we introduced *F. japonica* after 50 years in the reference scenario with only vegetative dispersal, henceforth called "low propagule pressure" (LPP) scenario, and (3) a scenario with similar settings as the low propagule pressure scenario but with added seed dispersal in autumn, henceforth called "high propagule pressure" (HPP) scenario (see section 3.3.1 for a detailed description on the dispersal mechanisms). The high propagule pressure can be seen as a hypothetical doom scenario where the invader is very persistent and abundant. Furthermore, we ran several scenarios with similar settings as the low propagule pressure scenario, but where we altered the mortality thresholds for flooding and desiccation, creating higher vegetation mortality and therefore less persistent invaders that more resemble a noninvasive riparian plant. In that way, a range of riparian species was simulated with different sensitivities to hydro-morphodynamic pressures. We additionally tested the sensitivity of the seed dispersal mechanism and the mortality of *F. japonica* in the high propagule pressure scenario, several scenarios have been run with different mortality thresholds and seeding densities. The model parameters for all scenarios are presented in Tables (2–4).

Table 2. Vegetation Parameters for *F. japonica*

Parameter	Unit	LPP[a]	HPP[a]	Reference
Maximum age	years	300	300	Continuous resprouting
Maximum shoot size	m	3	3	*Child and Wade* [2000]
Maximum rooting depth	m	3	3	http://www.kleerkut.co.uk/
Maximum stem diameter	m	0.05	0.05	*Hayen* [1995]
Stem density growing season	stems/m^2	80	80	G. Egger, personal communication, 2016
Stem density November/December	stems/m^2	40	40	G. Egger, personal communication, 2016
Start shoot growth	month	5	5	http://www.cornwallknotweed.org.uk/
End shoot growth	month	10	10	http://www.cornwallknotweed.org.uk/
Colonization window[b]	month	1–12	1–12/9–10	*Child and Wade* [2000]
Drag coefficient		1.5	1.5	Similar to older Salicaceae
Initial fraction[c]		0.1	0.1/0.8	EG[c]

[a]LPP is the low propagule pressure scenario, HPP is the high propagule pressure scenario.
[b]In both LPP and HPP scenarios there is year round colonization of *F. japonica* with a fraction of 0.1. Additionally, in the HPP scenario *F. japonica* colonizes two months in Autumn with a fraction of 0.8.
[c]EG is an educated guess.

Table 3. Mortality Parameters for Salicaceae Seedlings (1 Year Old), Saplings (2–10 Years) and Forest (Older Than 10 Years) in All Scenarios

Parameter	Unit	*Salix* Seedlings[a]	*Populus* Seedlings	*Salix* Saplings	*Populus* Saplings	*Salix* Forest	*Populus* Forest
Flooding threshold	*d*	40	35	230	220	310	290
Flooding slope		0.75	0.75	0.8	0.8	0.5	0.5
Desiccation threshold	*d*	15	20	170	180	365	365
Desiccation slope		0.75	0.75	0.3	0.3	1	1
Uprooting threshold	*m/s*	0.55	0.55	3.5	3.5	12.0	12.0
Uprooting slope		0.75	0.75	0.75	0.75	0.3	0.3

[a]For a visual example of this dose-effect relations see Figure 4.

3.2. Morphodynamic Model

Parametrization and initial bed level conditions of the morphodynamic model were similar to the model described in *van Oorschot et al*. [2016]. Additionally, we used measured daily discharges, as opposed to several generalized discharge curves, of the Allier River from 1968 to 1995 measured at the gauging station near the city of Moulins. We obtained a 300 year time period to sample from the discharge data that was available (27 years). We randomly sampled entire years of discharge data, such that the sequence of discharge years is random but flow seasonality within each year is maintained. After sampling, the discharges were averaged per month and subsequently used as input for the model. The monthly discharges ranged from a minimum value of 12 m^3/s in late summer to a maximum of 510 m^3/s in spring.

The initial conditions were composed of three sinus- shaped meander bends with similar dimensions to the Allier River. Delft3D (4.00.01) was used for morphodynamic calculations with shallow, depth-averaged flow conditions, sediment transport with Engelund-Hansen and bed level updates (for morphodynamic formulas, see *Lesser et al*. [2004]). Water flow was calculated with 12 s time steps, and bed level was calculated every 6 min, honouring the Levy-Courant condition. Delft3D is one of the worlds most advanced numerical morphodynamic models and has been successfully applied and validated in many studies [e.g., *Schuurman et al*., 2013].

3.3. Vegetation Model

The vegetation model was constructed in Matlab (R2013b) and comprises vegetation colonization, growth, prediction of hydraulic resistance, and mortality through flooding, desiccation, uprooting, scour and burial. The model contains an open structure where growth rules can be manually altered per species. This allows for easy adaptation of growth rules if the vegetation model would be coupled to a water quality model in the future. The structure of the vegetation model described in *van Oorschot et al*. [2016] was extended to include perennial plants with an *intra*-annual above-ground life-cycle, in addition to perennial plants with an *inter*-annual life-cycle, i.e., riparian trees. In the model, vegetation growth and mortality are calculated and updated in two-weekly time steps, as opposed to once a year in the previous version of the model. This results in a more dynamic and realistic system, because changes in morphodynamics directly affect vegetation processes and vice versa.

Table 4. Mortality Parameters for *F. japonica* for All Scenarios

Parameter	Unit	LPP[a]	HPP[a]	LPPa	LPPb	LPPc	LPPd	LPPe	LPPf	LPPg	LPPh	HPPi	HPPj	HPPk
Flooding threshold	*d*	300	300	275	250	225	200	175	225	200	175	175	175	300
Flooding slope		1	1	1	1	1	1	1	0.8	0.8	0.8	0.8	0.8	1
Desiccation threshold	*d*	365	365	365	365	365	365	365	175	150	125	125	125	365
Desiccation slope			1	1	1	1	1	1	0.3	0.3	0.3	0.3	0.3	1
Uprooting threshold	*m/s*	7	7	7	7	7	7	7	3.5	3.5	3.5	3.5	3.5	7
Uprooting slope		0.3	0.3	0.3	0.3	0.3	0.3	0.3	0.75	0.75	0.75	0.75	0.75	0.3

[a]LPP is the low propagule pressure scenario, HPP is the high propagule pressure scenario. The mortality parameters are similar for the LPP and HPP scenarios because they only differ in their colonization process. LPPa-LPPe are in order of decreasing tolerance for flooding, LPPf contains similar flooding, desiccation and uprooting parameters as the sapling phase averaged for *Populus and Salix* in the reference run. LPPg-h are derivatives from LPPf with increasing sensitivity for both flooding and desiccation HPPi is a HPP scenario with mortality boundaries of LPPh HPPj-k are HPP scenarios with mortality boundaries of LPPh and LPP respectively combined with an initial seeding fraction of 0.5.

All Salicaceae vegetation parameters were similar to the study described in *van Oorschot et al*. [2016] unless stated otherwise. Vegetation parameters for *F. japonica* were derived from literature and field experience (Table 2). Comparison of the simulation results of the model without invasive species to observed vegetation patterns along the Allier River demonstrated that the model yields realistic results, and is able to replicate typical vegetation and morphological patterns observed along this river [*van Oorschot et al*., 2016].

3.3.1. Colonization

Two colonization modules were implemented containing two different dispersal mechanisms; seed dispersal and vegetative dispersal. Seed dispersal was simulated by assuming seed deposition on bare substrate between the maximum and minimum water level within the seed dispersal time window. Seed dispersal was only active during the seed dispersal window and was characterized by a high initial fraction in each colonized grid cell. Vegetative dispersal was simulated by adding an additional morphodynamic activity requirement to the exposed bare substrate, which assumes that rhizome parts travel in sediment and can re-sprout when they are deposited on channel bars and banks. The morphodynamic activity was modeled as a minimum sedimentation threshold set to 1 *cm*, which corresponds to some morphodynamic activity necessary to transport the propagules to the corresponding location. Vegetative dispersal takes place year-round with small initial fractions at locations fitting both exposed bare substrate and morphodynamic activity requirements.

In all scenarios Salicaceae only disperse via seed dispersal (for parametrization, see *van Oorschot et al*. [2016]). The dispersal mechanism of *F. japonica* in the low propagule pressure scenarios is solely vegetative dispersal (Table 2). The high propagule pressure scenario combines both vegetative dispersal as well as 2 months of seed dispersal in autumn (Table 2).

The fraction of a certain species in a cell can increase each ecological time step when further colonization occurs in that cell. The fraction represents the area of the cell which is actually covered by vegetation, e.g., a fraction of 0.1 means that 10% of the cell contains vegetation with a given set of properties. A cell can contain multiple vegetation types or ages that are each represented by a certain fraction.

Cells are filled with a "first come, first serve" method which means that vegetation can colonize cells up to a maximum total fraction of one. This means that there is only competition for space included in the model, and not for e.g., light, moisture or nutrients. The magnitude and timing for filling the grid cells with vegetation, and hence competition for space, is therefore dependent on the timing of seed dispersal combined with the water levels during these periods, which determine where vegetation settles, and the initial density of grid cell occupation, that determines how fast a cell is fully occupied. Lateral vegetation expansion was not taken into account because we assume that this effect is minimal due to the relatively large cell size of 25 m x 25 m and the maximum lateral movement distance of up to 7 m/yr from the parent plant [*Child and Wade*, 2000].

3.3.2. Growth

Salicaceae species have an inter-annual growth cycle that is calculated using a logarithmic growth curve, which means that their shoot and root size increases every year (Figure 3a). They contain different life stages which differ in number of stems per m^2 and sensitivity for morphodynamic pressures [*van Oorschot et al*., 2016]. *F. japonica* has an intra-annual growth cycle, which means that the above-ground biomass starts to grow logarithmically in spring and dies off in winter, after which dead stakes remain present with half the stem density until the end of the calendar year (Figure 3b and Table 2). We assume that in the beginning of next year these stakes are removed by water or wind, since they are very brittle when dead. The rooting depth increases only logarithmically in the first year after colonization, so we assume that *F. japonica* reaches its maximum rooting depth already in the second year. This means that the below-ground biomass of established plants remains constant from the second year onward. The stem density of *F. japonica* is higher than the Salicaceae plants, representing denser vegetation.

Species growth rates are not affected by resource limitation or competition, e.g., shadowing and moisture availability. Groundwater access is not modeled explicitly, but is indirectly calibrated by setting higher desiccation thresholds for mortality, especially for older vegetation. We assume that these older vegetation types have sufficient access to groundwater during times of low flows, which is a valid assumption in lowland, sandy gravel rivers in cool temperate climatic zones. This assumption is not valid for rivers in more arid zones, where vegetation patterns are dominantly influenced by groundwater availability.

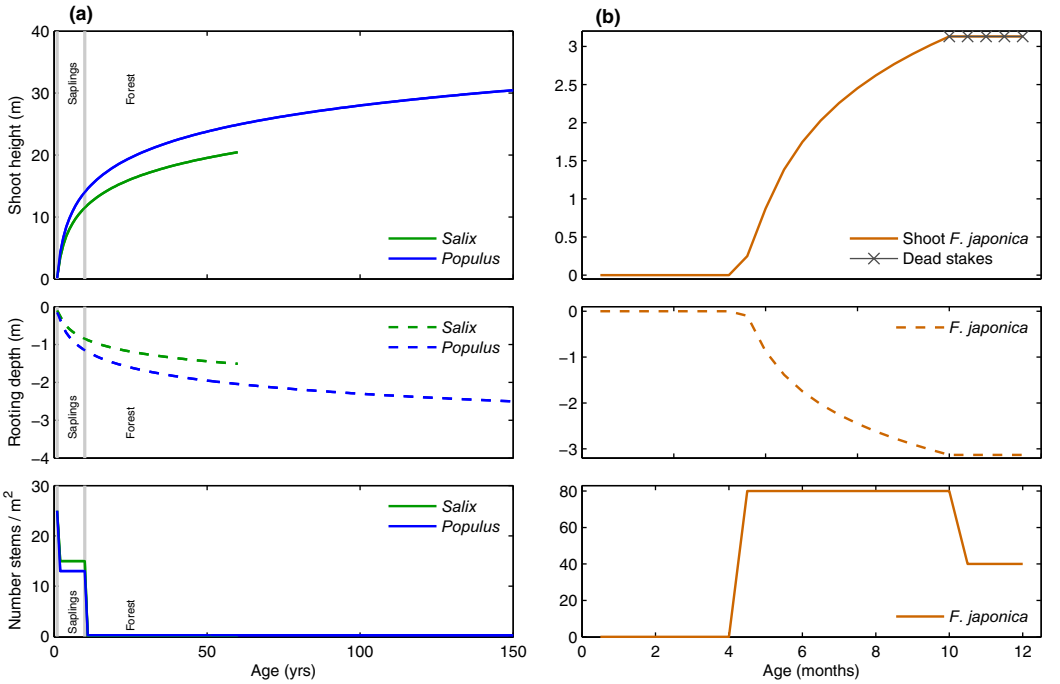

Figure 3. Growth curves of shoot height, rooting depth and number of stems per m^2 of Salicaceae species (a) and *F. japonica* (b). Note that graphs for Salicaceae and *F. japonica* have different vertical scales and that the growth of Salicaceae species is depicted per year while the growth of *F. japonica* is depicted per month. *F. japonica* roots only grow in the first year and keep their maximum depth from that point onward. Shoots resprout each calendar year, whilst the plant remains established, and keep half of their stems from the end of the growing season until the end of the calendar year.

3.3.3. Interaction

Vegetation interacts with hydro-morphodynamic processes by changing hydraulic resistance. This is dependent on the size of the vegetation, determining if water flows only through or also over the vegetation patch, and vegetation density, which is expressed by the stem diameter, the number of stems and the fraction with which vegetation occupies the cell. Hydraulic resistance caused by vegetation was calculated in each grid cell with the *Baptist et al*. [2007] relation:

$$C = \frac{1}{\sqrt{\frac{1}{C_b^2} + \frac{C_d n h_v}{2 \cdot g}}} + \frac{\sqrt{g}}{\kappa} \ln \frac{h}{h_v} \tag{1}$$

where C is the Chezy value of the vegetation $(m^{\frac{1}{2}}/s)$, C_b is the Chezy value for the un-vegetated parts, c_d is the drag coefficient, n is the vegetation density (stem diameter x number of stems per m^2), h_v is the height of the vegetation (m), h is the water depth (m), κ is the Von Karman constant (0.41) and g is the gravitational force (9.81 m/s^2). The Chezy value was calculated separately for each vegetation type (i.e., *Salix*, *Populus* and *F. japonica*) and age and subsequently the total sequential Chezy coefficient was calculated weighted by fraction coverage. The main differentiating parameters for native and invader vegetation parameters are the vegetation stem density, which is much higher for *F. japonica* than for the Salicaceae species, and vegetation height. In addition, these vary in different ways throughout the year when *F. japonica* grows (Figure 3b).

Sediment stabilization by roots was not explicitly taken into account. The current version of Delft3D uses a relatively simple bank erosion module that is not able to simulate detailed lateral bank erosion with processes like undercutting and bank failure of steep banks. Bank erosion takes place when a cell is incised and subsequently causes the neighbor cells to decrease 50% of the incised amount. However, because flow velocity is reduced within and behind vegetation patches, the amount of erosion in vegetated patches is automatically less.

3.3.4. Mortality

During a simulation, plants die through flooding, desiccation, uprooting, scour and burial depending on their sensitivity. For Salicaceae species, this is life-stage dependent, i.e., younger vegetation is more sensitive

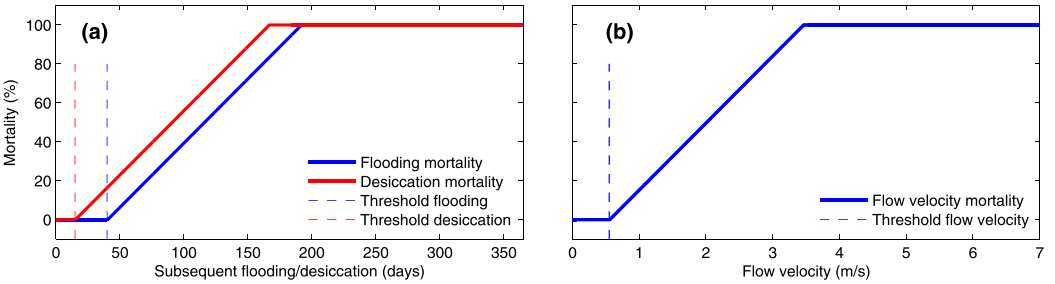

Figure 4. Dose-effect relations for *Salix* seedlings. (a) flooding and desiccation and (b) flow velocity.

to morphodynamic pressures. Plants that remain unaffected by morphodynamic processes die due to senescence when a predefined maximum age is reached. Flooding, desiccation and uprooting mortality is calculated with the dose-effect relation described in *van Oorschot et al*. [2016]; an example is given in Figure 4. The values of the thresholds and slopes in the dose-effect relations for Salicaceae species are presented in Table 3 and for *F. japonica* in Table 4. Because of the new model setup, the mortality thresholds were re-calibrated to approximate a total Salicaceae cover 15% after 150 years and an age distribution with a pioneer, bush and forest ratio of 0.2: 0.5: 0.3 (as in *Geerling et al*. [2006] and *van Oorschot et al*. [2016]). Burial occurs when the amount of sedimentation exceeds the shoot height and scour occurs when the amount of erosion exceeds the rooting depth. *F. japonica* has a very low sensitivity for flooding, desiccation and uprooting. It can die through burial, prolonged flooding or scour, particularly in the first year after colonization, because of the small rooting depth. Because it is continuously re-sprouting from rhizomes, we assume *F. japonica* does not die from senescence, unlike Salicaceae species.

3.4. Model Output Analysis

All model output was analyzed from year 51 onward, when the invader was introduced, to exclude the effect of initial morphodynamic conditions. To exclude boundary conditions, 500 *m* (20 grid cells) were trimmed off the upstream and the downstream boundaries of the morphodynamic and vegetation maps before statistics were calculated. As a measure of invasion speed, mean annual area increase of *F. japonica* was calculated between years and averaged over all years. Vegetated area was calculated as the total sum of all *F. japonica* fractions in occupied grid cells.

Because the slope of the invasion curve differs over time, the relative mean annual area increase was calculated for three separate stadia; the initial phase is defined as the minimum time needed to reach 50% of the maximum total covered area; the second phase is defined as the time needed to reach 80% of the maximum total covered area; the last phase is from the end of the second phase until the end of the run. See also Figure 8 for the total covered area over time and the corresponding invasion phases.

Vegetation covers were calculated as the percentage of grid cells occupied by vegetation of a certain age class relative to the total number of grid cells, independent of the fraction in the cell. The data were split into age classes of seedlings (1 year old), saplings (2 – 10 years old) and forest (vegetation older than 10 years), and combinations of different age classes occurring in the same cell.

The elevation ranges where colonization of vegetation had occurred were calculated by using histograms of the elevation distribution of vegetated cells on detrended bed level elevations related to mean initial bed level, for each year immediately after colonization. The histogram modes represent the bed level where most vegetation settles, i.e., the bin with the highest number. The intervals between the 10th and the 90th percentiles were calculated from all bed level bins containing vegetation. For representation of trends at longer timescales than individual floods, the plotted values were smoothed by taking the moving average over 10 years.

Mortality was calculated at each ecological time step for each selected age class and each morphodynamic pressure, and was represented as percentages of the total removed vegetation fractions. For visualization, the median mortality was calculated for each selected age class over time.

To show the relation between vegetation fraction in cells and bed level elevations, median bed level values for cells containing similar vegetation fractions were calculated at the end of the model run, in year 300.

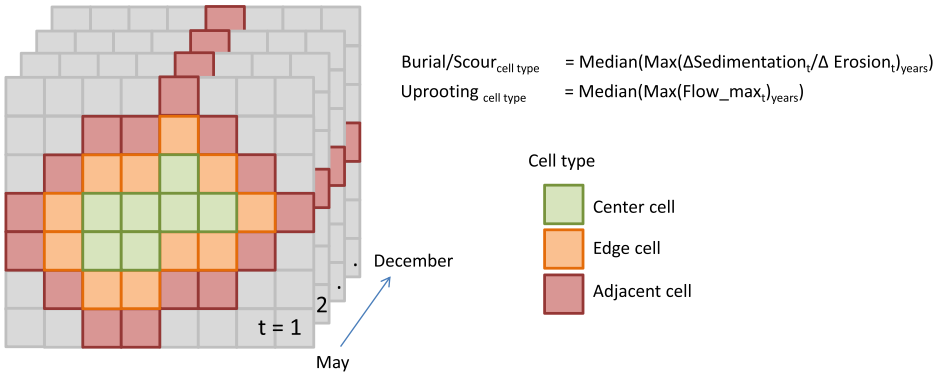

Figure 5. Method for the calculation of morphodynamics in center-, edge- and adjacent cells of a vegetation patch. Note that center- and edge cells define the vegetation patch and adjacent cells are just outside the vegetation patch.

This was done for cells with only Salicaceae species and cells with both Salicaceae species and *F. japonica*. To show the trend in bed level elevation where most vegetation settled, the values below −3 and above 2 meter have been clipped off.

Bed level statistics, maximum water levels, sediment transport, sinuosity and meander migration rate were calculated as described in *van Oorschot et al*. [2016]. To obtain statistics for an entire model run, median values of these statistics were calculated. For representation, data were smoothed by taking the moving average over 10 years.

Morphodynamic conditions in cell centers were calculated as the maximum sedimentation, maximum erosion and maximum flow velocity conditions for each ecological time step from the moment of colonization until the end of the calendar year in center-, edge- and adjacent cells of each vegetation patch (Figure 5). Edge and adjacent cells were determined by cells adjacent to the center- and edge cells respectively, diagonally adjacent cells were not taken into account. Vegetation patches were defined as grid cells containing vegetation older than 1 year. The morphodynamics per year over all ecological time steps were calculated as the maximum value per parameter. For representation, the values were smoothed by taking the moving average over 10 years.

4. Results

4.1. Vegetation Occupation and Expansion

Invasion of *F. japonica* affects both the spatial extent and distribution of native vegetation, expressed by the *number and location* of grid cells where native vegetation occurs, and the total areal cover of native vegetation, which also depends on the vegetation density *within* each grid cell.

Both invasion scenarios show a wide expansion of *F. japonica* (Figures 6b, 6c, 7b, and 7c), which in the high propagule pressure scenario leads to a reduction in spatial extent and areal cover of native Salicaceae vegetation. The final spatial extent of *F. japonica* is around 45% of the total area in the low propagule pressure scenario and 75% in the high propagule pressure scenario (Figures 7b and 7c), while the total areal cover, i.e., the absolute covered area of *F. japonica* is about 5 times higher in the high propagule pressure scenario (Figures 8a and 8b).

Invasion by *F. japonica* with high propagule pressure drastically decreases the median native vegetation extent by more than 10% (from 15% to 4%) already within 10 years after invasion, when compared to the reference scenario without invaders (Figure 7c). Remarkably, invasion with low propagule pressure increases the extent of Salicaceae species by almost 3%, to a total of 18% (Figure 7b). In fact, all scenarios with low propagule pressure show larger spatial extent of Salicaceae when compared to the reference scenario (Figure 9a and Table 6). However, within these scenarios there is a negative correlation between the *F. japonica* and Salicaceae extent: increasing *F. japonica* persistence (i.e., higher mortality thresholds) decreases occupation by native species (Figure 9a). The total covered area shows a similar trend: the low propagule pressure

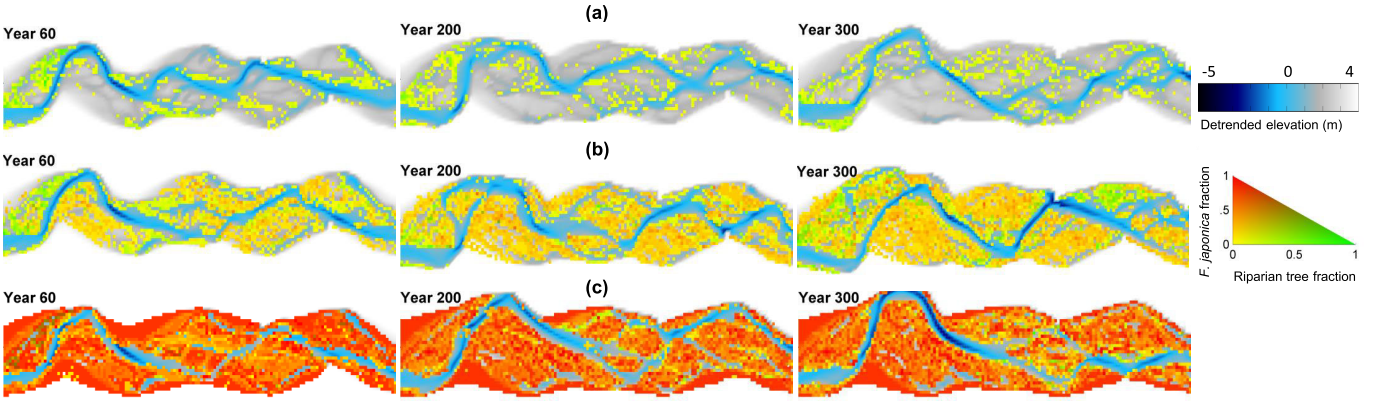

Figure 6. Bed level and spatial extent and distribution of vegetation extracted at the last ecological time step of three different years. (a) Reference scenario without alien plant invaders, (b) scenario with low propagule pressure of invasive alien plant species, (c) scenario with high propagule pressure of invasive alien plant species, at year (left) 60, (middle) 200, and (right) 300. The invader has been introduced in year 50. The vegetation color legend represents the cell occupancy (vegetation fraction within the cells) of both riparian trees and *F. japonica*. Bright green represents cells that are completely filled with riparian trees and red represents cells that are completely filled with *F. japonica*. All other colors are cells in which both vegetation types occur. The blue – gray legend is the detrended bed elevation, i.e., where slope and mean bed level was extracted from all bed level values.

scenario shows a higher areal cover of Salicaceae than the high propagule pressure scenario and the reference scenario (Figure 8c).

The relation between the total fraction of native and invasive vegetation *within* the grid cells (Figure 9b) shows a different trend for several high propagule pressure scenarios than the spatial extent (i.e., the *number of cells* occupied by vegetation) (Figure 9a). Both high propagule pressure scenarios with higher *F. japonica* mortality (HPPi and HPPj, Table 4), surprisingly show a larger *F. japonica* fraction within the cells, indicating a higher *F. japonica* density. Apparently, the final vegetation density within cells is not sensitive for the seeding fraction, that differs between 0.8 for HPPi and 0.5 for HPPj. Still, the combination of higher *F. japonica* mortality and lower seeding density (HPPj) results in less areal spread of *F. japonica* (Figure 9a). Sensitivity analysis on the seeding density and *F. japonica* mortality together with the high propagule pressure scenario thus revealed that seeding density is not the sole driver of *F. japonica* spread and density. Only lower seeding density combined with increased mortality decreases *F. japonica* spread. When only

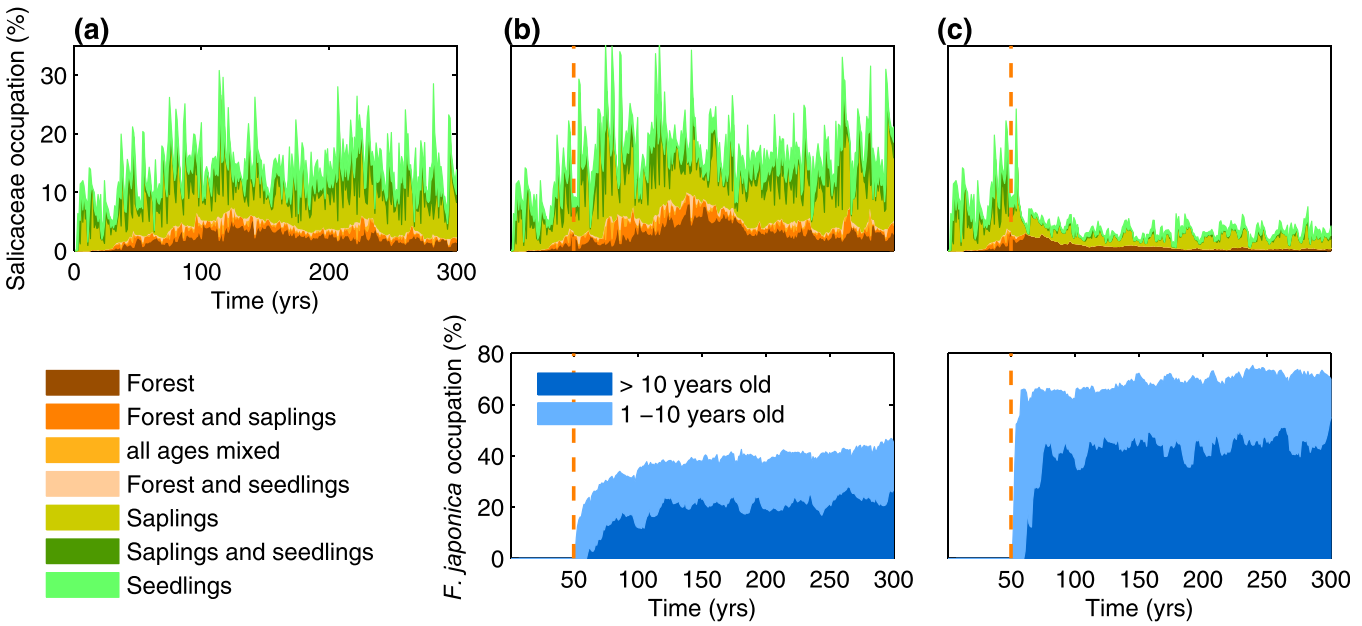

Figure 7. Spatial extent of Salicaceae species (top graphs) and *F. japonica* (bottom graphs) over time. (a) Reference scenario with only Salicaceae species, (b) low propagule pressure scenario, (c) high propagule pressure scenario. The striped line indicates the start of the invasion. Seedlings are up to 1 year old plants, saplings are plants between 2 and 10 years old and forest consists of trees older than 10 years.

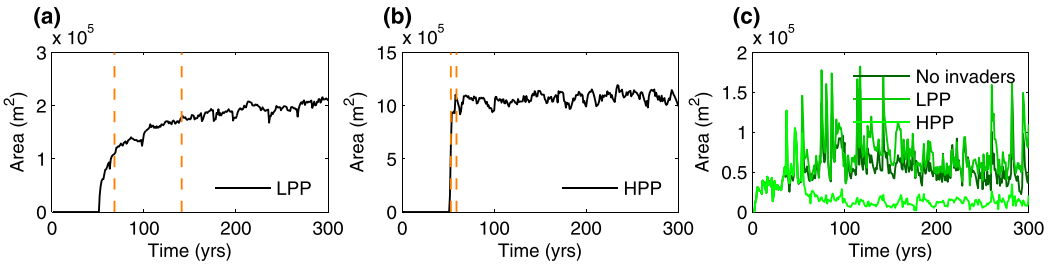

Figure 8. Absolute areal cover of Salicaceae and *F. japonica* over time. (a) Total *F. japonica* area in the low propagule pressure scenario (LPP), (b) total *F. japonica* area in high propagule pressure scenario (HPP), (c) total Salicaceae area in three main scenarios. The boundaries for the time frames of the invasion phases in Table 5 are depicted as orange striped lines.

seeding density is lowered, i.e., in the HPPk scenario, results do not differ from the main HPP scenario. Furthermore, the native vegetation extent and fraction is not increasing when either seeding density or mortality of *F. japonica* is altered. This suggests that there is only a small "window" in the *F. japonica* dispersal and mortality parameter range where native vegetation is facilitated.

In both invasion scenarios, areal cover increase of *F. japonica* occurs in several phases (Figures 8a and 8b). It starts with a rapid colonization where *F. japonica* occupies all available niches, followed by a slower expansion where remaining niches are filled as soon as hydro-morphological conditions are favorable. This mean area increase per phase is calculated by the difference in relative invaded areal cover between years, and is summarized in Table 5.

The initial phase, defined here as the minimum time needed to reach 50% of the maximum areal cover, takes fewer years in the high propagule pressure scenario, where the increase is very steep in the first year after invasion, while this phase takes 16 years in the low propagule pressure scenario (Figures 8a and 8b). A similar difference is found for the second phase, defined here as the minimum time needed to reach 80% of the maximum areal cover, which is already reached within 10 years in the high propagule pressure scenario and after almost 90 years in the low propagule pressure scenario. In the low propagule pressure scenario, the invaded area continues to increase, while in the high propagule pressure scenario the niches are almost fully occupied already within the first two phases, where after the occupied area shows a dynamic equilibrium. The increase of area occupied by Salicaceae does not show a typical increasing trend, but varies throughout the model run in all scenarios (Figure 8c).

4.2. Vegetation Colonization and Mortality

The detrended elevation range where most Salicaceae species colonize lies between 0 and −1 meter relative to mean initial bed level, is similar in all main scenarios, and remains unchanged during the runs (Figure 10a). However, the total bed level range where colonization occurs increases toward higher elevations during the runs for the reference scenario and for the low propagule pressure scenario. This suggests that the landscape is becoming more heterogeneous and water is able to carry the seeds higher up the floodplain.

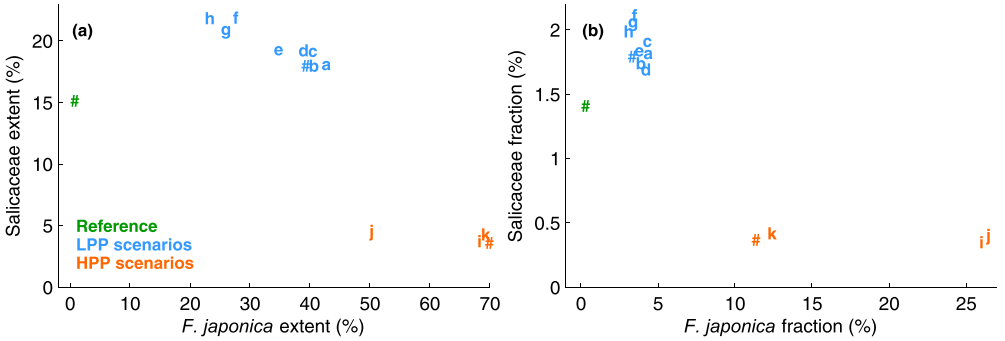

Figure 9. Relation between the median spatial extent (a) and fraction (b) for Salicaceae and *F. japonica* for all age classes combined. LPP: low propagule pressure scenarios with different persistence, # is the main scenario, HPP: high propagule pressure scenarios, # is the main scenario. (see Table 4 for parameter settings and letter abbreviations). Values have been slightly adapted to prevent overlapping of letters, precise values can be found in Table 6.

Table 5. Relative Mean Annual Area Increase of *F. japonica* in Different Phases of the Invasion

Phase[a]	Parameter	Unit	LPP	HPP
Whole run	Mean increase	%/yr	0.88	1.5
	Maximum increase	%/yr	56	309
Initial phase	Time frame	years	52–68	52–53
	Mean increase	%/yr	9	309
	Maximum increase	%/yr	56	309
Second phase	Time frame	years	69–141	54–59
	Mean increase	%/yr	0.68	3.1
	Maximum increase	%/yr	8.9	19
Last phase	Time frame	years	142–300	60–300
	Mean increase	%/yr	0.13	0.02
	Maximum increase	%/yr	7.7	12

[a]For explanation of invasion phases see the Method section. LPP:low propagule pressure, HPP: high propagule pressure.

In this way, more locations become available for colonization. Contrastingly, the high propagule pressure scenario does not show an increase in colonization range for Salicaceae. A similar pattern is found for vegetation survival (Figure 10b). In the high propagule pressure scenario, the bed level elevation where most seedlings survive is a little higher than in the reference scenario and the low propagule pressure scenario. This indicates that fewer seedlings can survive at lower elevations on the floodplain where morphodynamic pressures are higher. This result is confirmed by the high mortality due to burial, scour and flooding in this scenario (Figure 12). However, the bed level elevations where most seedlings colonize and survive differ very little between scenarios compared to the total bed level elevation ranges where vegetation settles and survives. This range shows the confinement of seedlings due to either morphodynamic pressures at lower bed level elevation side or biotic pressures at the higher bed level elevation side. In the high propagule pressure scenario the development of seedlings is mainly restrained at the high bed level elevation side. This suggests that the limited expansion in elevation is because these habitats have become unavailable due to a rapid and dense *F. japonica* development.

Total vegetation densities *within* the cells are the largest in the high propagule pressure scenario (Figure 11c), and range up to the maximum value of 1.0 for fully occupied cells. Furthermore, higher vegetation densities occur at higher elevations. Figure 6c shows the bright red areas with high densities of *F. japonica* on the higher parts of the floodplain. In this scenario most cells are occupied with a dense *F. japonica* cover, with a much smaller fraction of the cells covered by Salicaceae species. This confirms the inference made above that colonization and survival of Salicaceae are hampered by the lack of suitable sites because they are already fully utilized by *F. japonica*. However, the low propagule pressure scenario shows an opposite trend where higher densities of both Salicaceae and *F. japonica* seem to occur at lower elevations and Salicaceae species are generally the most dominant species within the cells. These areas with dense areal cover of Salicaceae are visible as the bright green patches in Figure 6b. Compared to the reference scenario, the native Salicaceae species in both invader scenarios occur with larger range of densities (Figures 11b and 11c): for the high propagule pressure the maximum fraction of Salicaceae is 0.8 and for the low propagule pressure scenario 0.65, while it is 0.45 for the reference scenario. This indicates that inclusion of an additional species can locally increase the density of Salicaceae occupation.

The invader not only affects colonization of the native species, but also has an indirect effect on the mortality of the natives. All low propagule pressure scenarios show a reduced Salicaceae mortality for burial, scour and uprooting, when compared to the reference scenario (Figure 12: Mortality scenario/Mortality reference < 1). In contrast, the high propagule pressure scenario shows a higher mortality due to scour, burial and flooding, and a lower mortality due to uprooting and desiccation. The summed seedling mortality for all pressures is smaller in all *F. japonica* scenarios than in the reference. This shows that introduction of *F. japonica* reduces mortality for Salicaceae species independently of the invaders persistence.

Vegetation patches are generally larger in the invader scenarios than in the reference scenario (Figure 6). We hypothesize that these patches alter local morphodynamic conditions within and around patches, which, in turn, enhances vegetation settlement and survival. To test this, we extracted the morphodynamic conditions, i.e., erosion, sedimentation and flow velocities within and around the vegetation patches. To compare the effects of different colonization locations on vegetation survival we subdivided patches into i)

AGU Water Resources Research

10.1002/2017WR020854

Table 6. Morphodynamic and Vegetation Statistics[a]

Parameter	Unit	Ref	LPP	HPP	LPPa	LPPb	LPPc	LPPd	LPPe	LPPf	LPPg	LPPh	HPPi	HPPj	HPPk
5P Sal cover	%	9.7	12.7	1.9	11.9	12.0	12.7	12.9	12.8	14.2	13.6	14.3	2.2	2.8	2.2
50P Sal cover	%	15.2	18.0	3.6	18.1	18.0	19.2	19.3	19.4	21.9	21.0	21.9	3.8	4.6	4.3
95P Sal cover	%	24.1	29.3	6.5	27.9	30.0	29.2	28.5	31.2	35.5	34.9	35.2	7.2	9.1	7.9
50P Sal fraction	%	1.4	1.8	0.4	1.8	1.8	1.9	1.7	1.8	2.1	2.1	2.0	0.4	0.4	0.4
5P *F. jap.* cover	%	0.0	23.8	62.4	22.4	22.3	21.2	24.0	21.6	21.0	19.7	17.1	62.4	45.0	62.9
50P *F. jap.* cover	%	0.0	39.0	69.2	41.9	39.8	39.0	38.1	34.0	27.2	25.2	22.5	67.9	49.9	68.5
95P *F. jap.* cover	%	0.0	44.0	73.7	48.2	42.8	43.4	42.9	39.0	33.6	33.5	28.2	73.8	55.2	73.1
50P *F. jap.* fraction	%	0.0	3.3	11.1	3.8	3.5	3.5	3.6	3.5	3.3	3.0	2.8	25.8	26.3	12.1
5P Bed level	m	−2.6	−2.5	−2.7	−2.7	−2.6	−2.7	−2.7	−2.7	−2.7	−2.6	−2.5	−2.6	−2.4	−2.5
50P Bed level	m	0.05	−0.07	−0.06	−0.14	−0.14	0.01	−0.11	−0.14	−0.11	−0.01	−0.01	−0.04	−0.09	−0.16
5P Transport	$m^3/s/m$	2.9×10^{-10}	5.8×10^{-11}	2.7×10^{-12}	7.6×10^{-11}	8.9×10^{-11}	9.8×10^{-10}	1.1×10^{-10}	1.2×10^{-10}	1.6×10^{-10}	1.6×10^{-10}	1.7×10^{-10}	1.2×10^{-12}	5.6×10^{-12}	3.5×10^{-12}
50P Transport	$m^3/s/m$	4.2×10^{-7}	2.0×10^{-7}	5.3×10^{-8}	2.2×10^{-7}	2.2×10^{-7}	2.3×10^{-7}	2.2×10^{-7}	2.5×10^{-7}	2.3×10^{-7}	2.2×10^{-7}	2.2×10^{-7}	3.0×10^{-8}	7.5×10^{-8}	6.5×10^{-8}
95P Transport	$m^3/s/m$	1.8×10^{-5}	1.5×10^{-5}	1.4×10^{-5}	1.4×10^{-5}	1.3×10^{-5}	1.3×10^{-5}	1.4×10^{-5}	1.3×10^{-5}	1.3×10^{-5}	1.3×10^{-5}	1.4×10^{-5}	1.1×10^{-5}	1.4×10^{-5}	1.3×10^{-5}
50P Sinuosity		1.30	1.34	1.57	1.51	1.45	1.42	1.41	1.42	1.42	1.36	1.38	1.38	1.46	1.62
50P Migration rate	m/yr	66	70	68	80	86	80	77	73	88	81	79	44	87	62

[a]Ref = reference (Table 3), HPP = high propagule pressure, LPP = low propagule pressure and LPPa-h = low propagule pressure scenarios, HPPi-k = high propagule pressure scenarios (Table 4). 5P = 5th percentile, 50P = median, 95P is the 95th percentile.

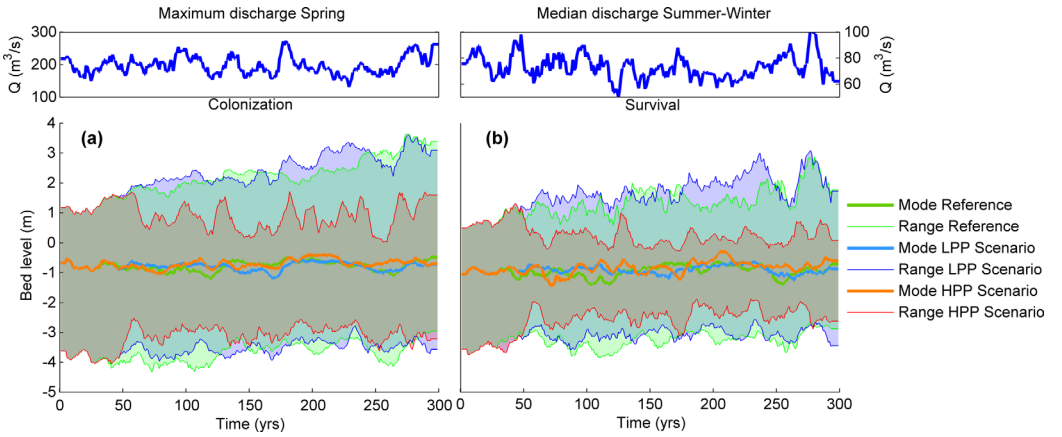

Figure 10. (a) Colonization range of Salicaceae seedlings on bed level related to mean initial bed level. (b) Survival range of Salicaceae seedlings on bed level related to mean initial bed level. The middle lines are the locations where most vegetation colonizes (mode). The shaded areas visualize the bed level ranges between the 10th and the 90th percentiles. The most important discharges for the depicted processes are shown on top. For colonization that is the maximum discharge in spring during the seed dispersal window to give an indication for the establishment range. For survival that is the median discharge for the rest of the season, i.e., from July until December, giving an indication for flooding and desiccation after colonisation.

center cells that are completely surrounded by other vegetated cells, ii) edge cells that are on the boundary of the vegetation patch, and also identified iii) unvegetated cells adjacent to the vegetation patch. These cells adjacent to vegetation experience the most hostile conditions, i.e., the highest morphodynamic activity, for Salicaceae settling, while conditions in the center cells are least hostile (Figures 13a–13c). In the reference scenario, most Salicaceae seedlings colonize in adjacent or edge cells, and very few in center cells (Figure 13d). However, in both invader scenarios, most Salicaceae seedlings colonize in edge cells, and in the high propagule pressure scenario also in center cells (Figures 13e and 13f). This effect is due to the

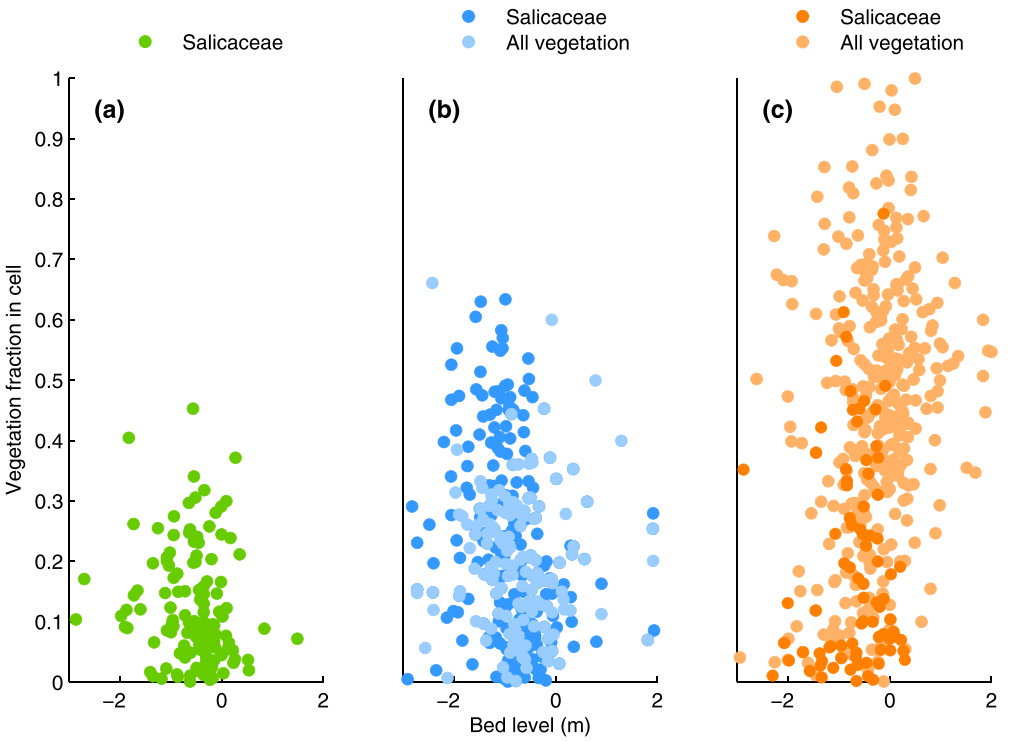

Figure 11. Fractions of vegetation occupancy within cells related to detrended bed level elevation at year 300. (a) Reference scenario, (b) low propagule pressure scenario and **c)** high propagule pressure scenario.

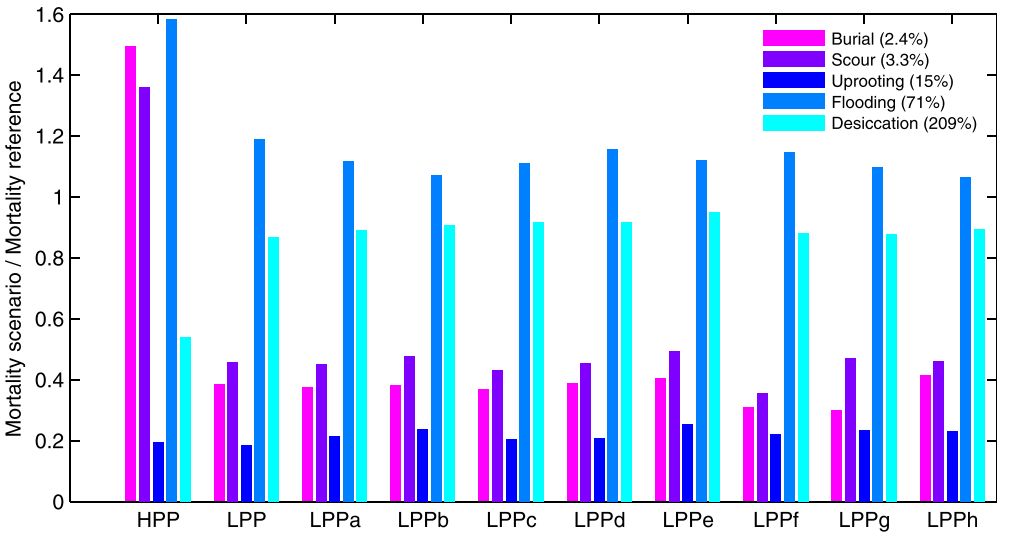

Figure 12. Mortality of Salicaceae due to all modeled morphodynamic pressures for all scenarios expressed as a fraction of the mortality of the reference scenario. Values $>$ 1.0 indicate a higher mortality than the reference. The values between the parentheses in the legend give the original mortality values of the reference scenario. Values can exceed 100% because mortality is calculated cumulative. See Tables 6 and 4 for explanations on scenario acronyms.

larger size of vegetated patches in the invader scenarios, increasing the number of available edge and center cells. In the low propagule pressure scenarios the morphodynamic conditions at colonization sites are lower than in the reference scenario, indicating a shielding effect. Contrastingly, In the high propagule pressure scenario the conditions at colonization sites are more hostile compared to the other scenarios, showing the largest amount of erosion and sedimentation and the highest flow velocities.

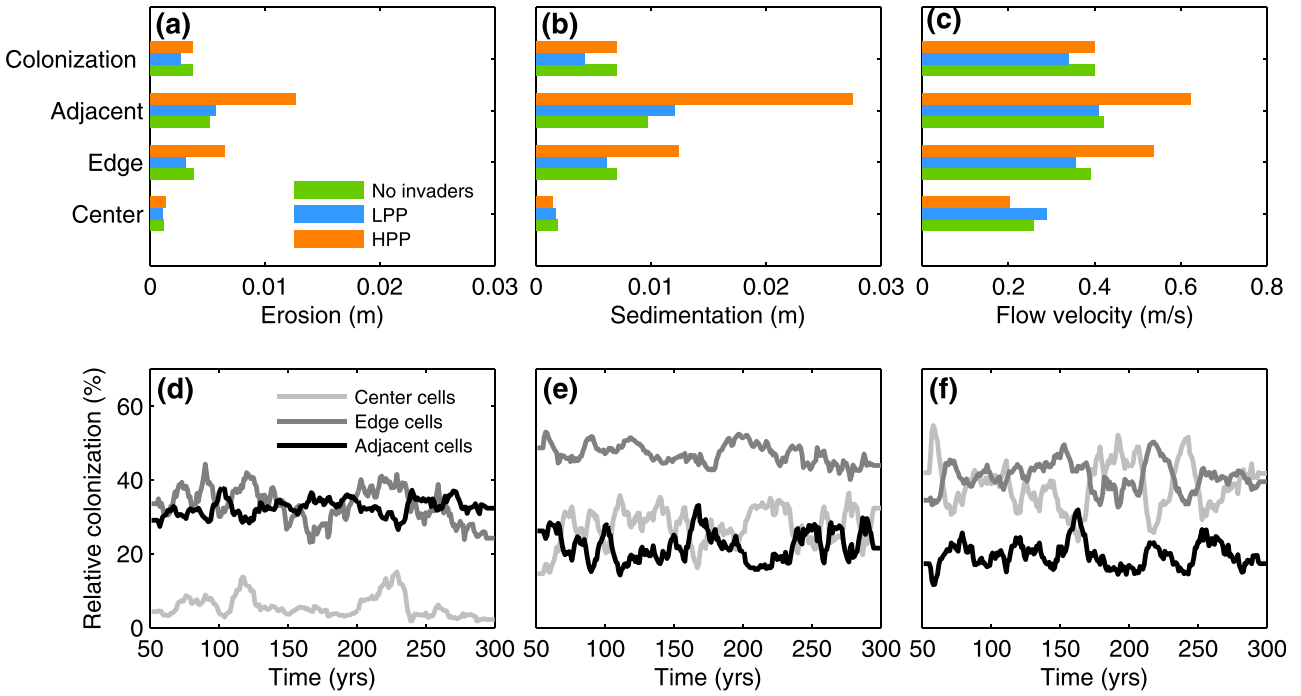

Figure 13. Morphodynamic conditions and the relative amount of colonization of Salicaceae in and around vegetation patches. (a) Median values for maximum erosion, (b) maximum sedimentation and (c) maximum flow velocities in center cells surrounded by other vegetation, edge cells located on the boundary of a vegetation patch, adjacent cells located just outside the vegetation patch, and average conditions for all locations where seedlings colonize. (d) Relative percentage of Salicaceae seedlings colonizing in center, edge or adjacent cells, expressed as percentage of total vegetated area for the reference scenario (e) low propagule pressure (LPP) scenario and (f) high propagule pressure (HPP) scenario.

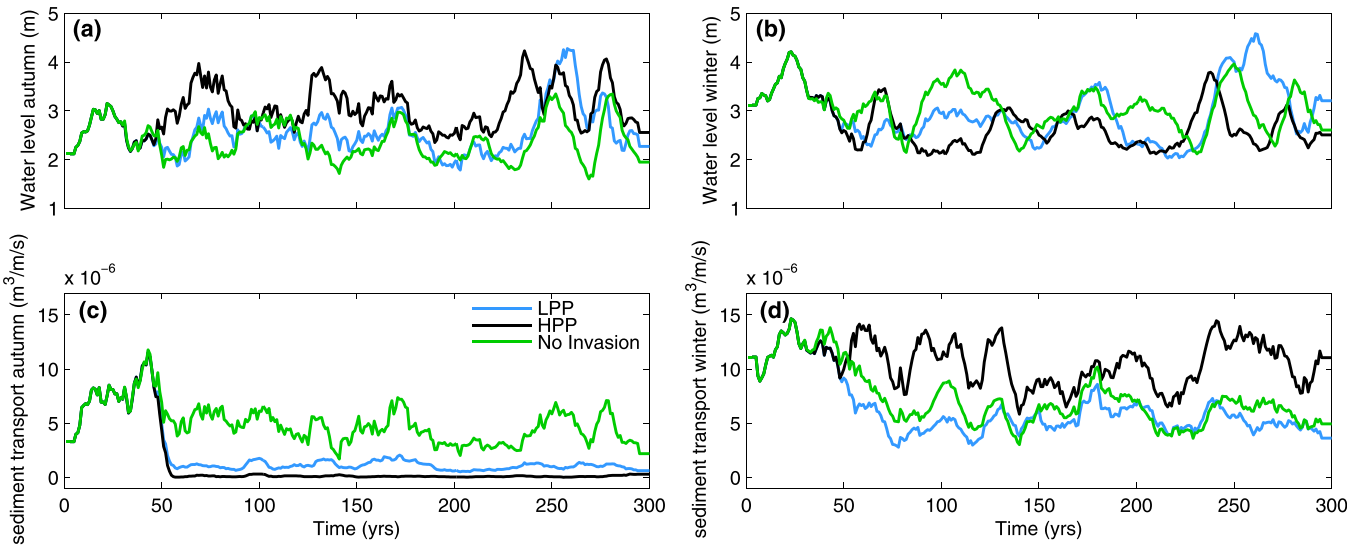

Figure 14. (a) Maximum water level in autumn, (b) maximum water level in winter, (c) 95th percentile of sediment transport in autumn, (d) 95th percentile of sediment transport in winter. LPP: low propagule pressure; HPP: high propagule pressure.

In summary, we predict a general lower Salicaceae seedling mortality in the invader scenarios with low propagule pressure due to a shielding effect of present vegetation on establishing seedlings, while the mortality of seedlings in the high propagule pressure due to intensified hydro-morphodynamic pressures at colonization sites increases.

4.3. Morphodynamics

There is a clear relation between vegetation occupation and sinuosity in all scenarios, where a larger and denser vegetation cover leads to a higher sinuosity. Furthermore, the denser vegetation in all invader scenarios reduces sediment transport and results in a slightly lower bed level, indicating that on average, the floodplain is slightly incising compared to the reference scenario. Still, the scenarios do not show large differences in morphodynamics in terms of river planform or average morphodynamic statistics (Table 6). All show a dynamic meandering river with downstream migration of meander bends and cut-offs (supporting information Movies S1–S3). The high propagule pressure scenario, resulting in the largest and most dense overall vegetation cover shows the largest sinuosity and lowest sediment transport rates (Table 6 and Figure 6). Water levels are affected by vegetation location, extent and density, which vary from year to year, and during the year. In the high propagule pressure scenario there is a large difference between maximum water levels and sediment transport rates in autumn, when *F. japonica* is at its tallest, and winter, when the above-ground biomass of *F. japonica* has disappeared (Figure 14). In this scenario, water levels are much higher in autumn than in winter, while the discharges in winter are generally higher (Figures 14a and 14b). When *F. japonica* development is most dense, there is a large backwater effect, while in winter, when the above-ground biomass of *F. japonica* is gone, this effect is diminished, leading to relatively low water levels compared to the low propagule pressure scenario and the reference scenario (Figure 14b). Furthermore, in the high propagule pressure scenario, the 95th percentile of the sediment transport is almost zero in autumn, while it is the highest of all scenarios in winter. This seasonal difference in sediment transport is due to the large reduction of Salicaceae species, which maintain more of their above-ground biomass in winter. The high propagule pressure scenario has less Salicaceae cover and therefore shows more bare substrate in winter, leading to higher sediment transport rates, and thus larger seasonality in sediment transport (Figures 14c and 14d).

4.4. Comparing Model Data to Field Data

In the absence of long-term data for *F. japonica* expansion on the floodplains of the Allier River we compare our model results to spatial expansion data of *F. japonica* along the Schwechat river. Although these rivers differ in size and activity (see section 2), we see similar spatial expansion behavior when we compare two relatively similar shaped meander bends (Figures 15a and 15b). Also, the temporal pattern of range

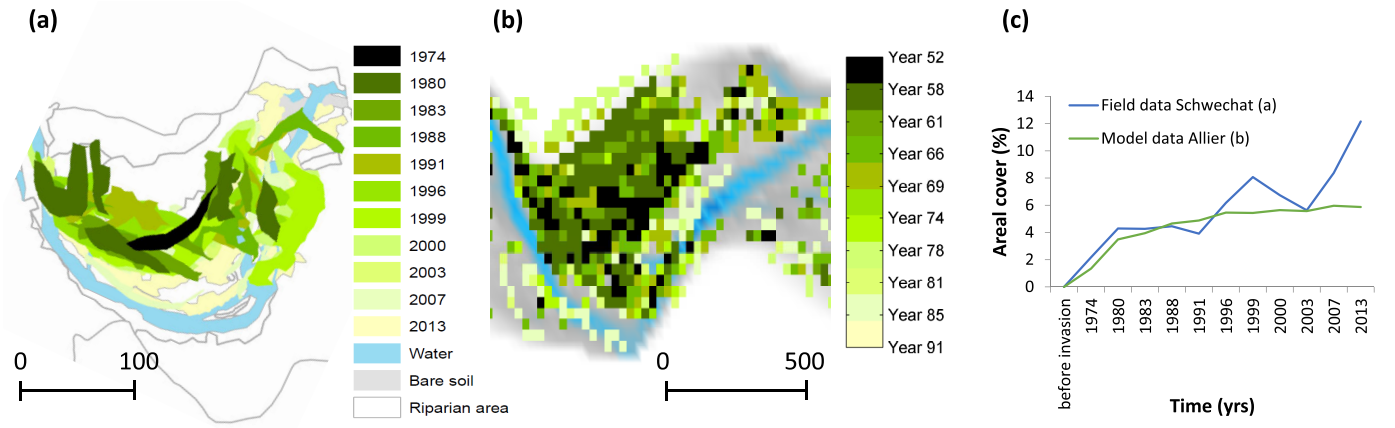

Figure 15. (a) Comparison of spatial *F. japonica* expansion of field data along the Schwechat River and (b) modeled data for the Allier River for several years, representing grid-cells where *F. japonica* is dominant. (c) Statistics for areal cover over time relative to the total riparian area for both rivers. In the model results, *F. japonica* cover was calculated with the total summed fractions within the grid-cells representing the total vegetated area.

expansion shows that the areal cover over time, relative to total riparian area, falls within a similar order of magnitude for both rivers (Figure 15c).

5. Discussion

5.1. Conceptual Model

This study investigates general emergent patterns in vegetation and hydro-morphodynamics generated by idealized model runs. The main insights from this study have been captured in a conceptual model. Figure 16 shows the main interactions between vegetation and hydro-morphodynamics that have been modeled in this study (Figure 16a) and the results of these interactions for three stages with increasing levels of invader abundance (Figure 16b). Through variations in model parameters for the invader scenarios, we seek to extend this work beyond a particular species and a particular case study. However, due to limited field data on long-term interactions between native plant species, invasive alien species and hydro-morphodynamic processes in river floodplains to validate our model outcome, the results from this study have primarily an explorative character. Obviously, an important recommendation from this research is to monitor vegetation establishment, vegetation succession and alien-native plant interactions under various hydro-morphological conditions and river management regimes. Nevertheless, our model results can be compared to some extent to field data from other rivers with different size and dynamics as well as conceptual models and theory from literature. We have shown that the modeled spatial expansion of *F. japonica* along the Allier is in general agreement with field data from the Schwechat River (Figure 15). In both rivers *F. japonica* establishes when conditions are favorable and might subsequently expand around the original stand due to combined effects of eco-engineering properties of the plants, creating more favorable conditions for settlement, and the availability of new substrate due to river migration and cut-offs. Also, the invasion speed of *F. japonica* falls within the ranges reported in literature (Table 5). This ranges from 15% mean relative annual increase in the heavily modified river Saar [*Vollmer*, 2012] to 0.3% in a natural reach of the Schwechat River [*Gruener*, 2016]. Our model results show an increase of 0.88% for the low propagule pressure scenario and 1.5% for the high propagule pressure scenario (Table 5). All other scenarios with less persistent invaders show a lower invasion speed when compared to the high propagule pressure scenario; overall, we find invasion speed to increase along with invader persistence. These results show that the model is able to reproduce behavior we see in the field. We further explore model validity by comparing patterns and dynamics predicted by the model to information from the literature. Below we discuss the three main insights from this study:

1. Persistent, abundant invaders decrease native vegetation cover by out-competing them, shifting accessible colonization sites toward lower floodplain elevations and increasing hydro-morphodynamic pressures at these sites, i.e., effect of propagule pressure on invasion impact.

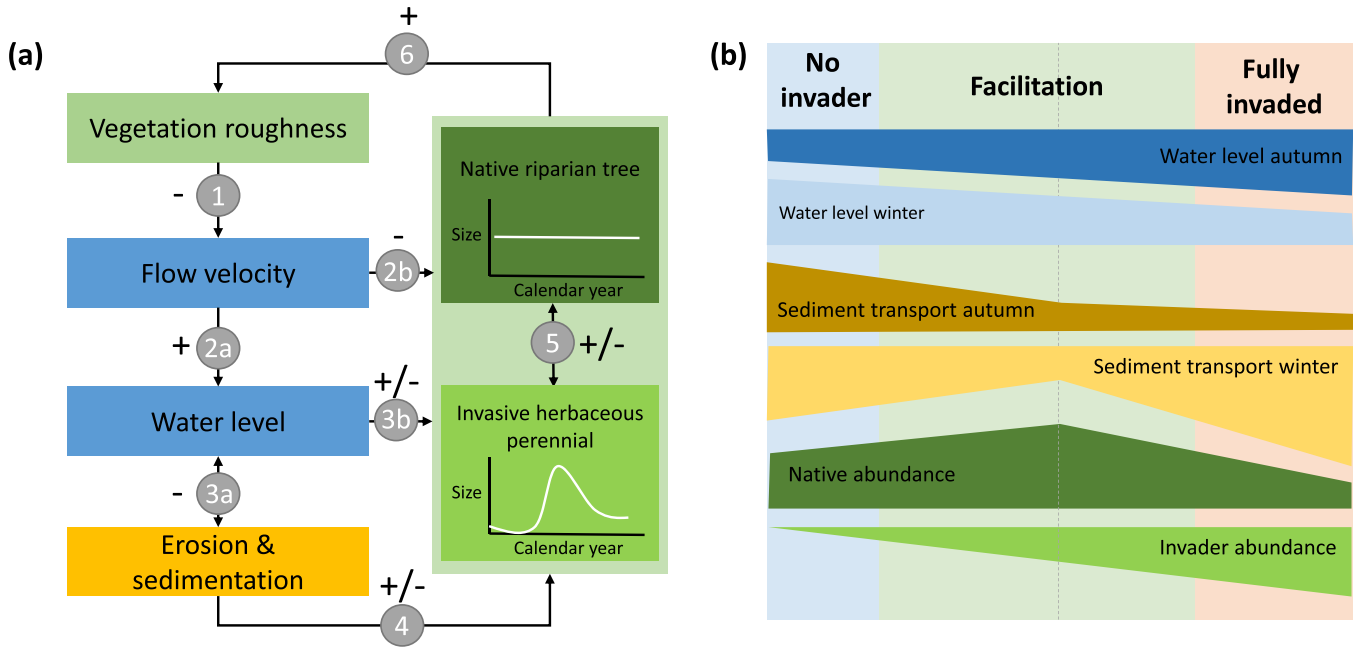

Figure 16. Conceptual model of the main modeled processes, interactions and scenario results. (a) Main processes and interactions between vegetation and hydro-morphodynamics included in the model. 1: Increasing vegetation roughness decreases flow velocity, which in turn elevates water levels due to backwater effects (2a). Additionally, flow velocity can cause uprooting of vegetation (2b). Increasing water levels and reduced flow velocity in vegetated patches decrease the morphodynamic activity by reducing erosion and sedimentation (3a), which in turn can have positive effects on vegetation by creating suitable new conditions for settlement or negative effects through burial and scour next to vegetated patches (4). Increasing water levels can either be positive for vegetation development due to moisture supply or increasing the area suitable for vegetation settlement, or negative through increased flooding mortality (3b). Vegetation interacts through competition for space (5) and affects total vegetation roughness based on their abundance and characteristics, that differ between years for native riparian trees and within the year for invasive herbaceous perennials (6). (b) Overview of seasonal effects of invasion intensity on water level, sediment transport and native vegetation in three stages; 1. natural system without invader, 2. facilitation with low invader abundance, 3. fully invaded system with high invader abundance and persistence. Explanations of these results are offered in the main text.

2. Less abundant and less persistent invaders facilitate native vegetation development by creating favorable hydro-morphodynamic conditions at colonization sites through shielding, i.e., facilitation of native species by invaders.
3. Seasonal, dynamic properties of invaders and native species determine hydro-morphodynamic invasion effects, i.e., seasonal bio-morphodynamic invasion effects.

5.2. Effects of Propagule Pressure on Invasion Impact

The invasion scenario with high propagule pressure shows a strong decline in total areal cover and spatial extent of native vegetation. This is caused by fast occupation of available open niches by highly persistent invaders that occur abundantly (Figure 7 and Table 5). Especially at more elevated locations on the floodplain where morphodynamic pressures do not eliminate the invader, the dense invasive vegetation leaves less room for development of Salicaceae species (Figure 6 and Figure 11). This strong competition for space leads to a smaller elevation range for colonization of native species at lower elevations with higher morphodynamic pressures and consequently a higher mortality due to burial, scour and flooding (Figures 10 and 12). The morphodynamic pressures at colonization sites are relatively high compared to the other scenarios (Figures 13a–13c). This could be attributed to the dense vegetation patches that divert and accelerate the flow between vegetated patches. This behavior is commonly seen in tidal marshes where the flow is concentrated between laterally expanding vegetation patches thereby leading to channel erosion [*Temmerman et al.*, 2007].

Due to decreasing area of suitable colonization niches for native species, there is no rejuvenation of vegetation, initially leading to aging and eventually a total decline of native riparian vegetation (Figure 7c). This result confirms the hypothesis that *Fallopia* species could alter the course of forest development, thereby affecting structure and functioning of terrestrial and aquatic habitats [*Urgenson et al.*, 2014]. This effect is also visible in floodplains of the Schwechat River, where *F. japonica* development strongly reduces

Salicaceae recruitment (Field observation by Dr. G. Egger), and also preliminary results from *Aguilera et al*. [2010] confirm that *F. japonica* can suppress regeneration of forest.

The niche available for invasion by alien plant species in our model is large due to the lack of a natural vegetation cover other than Salicaceae species. This creates much suitable habitat for *F. japonica* which in reality could be occupied by herbaceous vegetation and grassland, such as is actually the case in riparian areas along the Allier River. Furthermore, *F. japonica* growth is dependent on the availability of disturbed, open substrate, and it is reduced when shaded by other vegetation [*Beerling et al*., 1994]. Not including other native species than the main ecosystem engineers in the scenarios may cause bias of our model toward higher susceptibility for invasion. Biotic resistance, i.e., the ability of native species to prevent dominance of invasive species can sometimes be overcome by a high propagule pressure of invaders [*Berg et al*., 2016]. This has also been illustrated by the difference between our low and high propagule pressure scenarios. *Bimova et al*. [2004] showed that species richness of the invaded community does not influence invasion success of *Fallopia* species, and that environmental conditions and propagule spread are more important. *Lockwood et al*. [2005] also attribute establishment success to high propagule pressure, and state that with increasing disturbance, lower propagule pressure is needed for successful establishment of invaders. Our simulation results show that a high propagule pressure can indeed contribute to invasion success. Obviously, our high propagule pressure scenario is extreme. Nevertheless, a similar effect of displacement of cottonwoods by *F. japonica* is also visible in the Schwechat River at a local scale, suggesting that this large-scale and disproportionate effect in the high propagule pressure scenario may indeed be realistic at specific locations. Thus, given that the human-induced climate change increases the distribution range of *F. japonica* and its hybrids, and that some of these hybrids spread even faster than their parents and also produce viable seeds [*Groeneveld et al*., 2014], our high propagule pressure case appears to be a plausible scenario for the future.

5.3. Facilitation of Native Species by Invaders

Our model results show that established vegetation of Salicaceae as well as *F. japonica* facilitates the survival of Salicaceae seedlings by reducing the morphodynamic pressures inside and around vegetation patches. Morphodynamic conditions are least hostile within vegetation patches, but become more intense toward the edge and outside of a patch (Figures 13a–13c). Eco-engineering species can have a positive feedback on their own development and can create beneficial conditions for other species as well [e.g., *Odling-Smee et al*., 2013; *Gurnell*, 2014; *Corenblit et al*., 2016]. Facilitation is a natural part of the sequence of vegetation phases that interact with water and sediment, or "biogeomorphic succession" [*Corenblit et al*., 2007]. This starts with bare substrate that is colonized by pioneer seedlings and over time evolves toward more resistant vegetation that is capable of actively influencing hydro-morphodynamic conditions and hence river pattern. During these latter succession phases the landforms containing these vegetation patches experience less hydro-morphodynamic pressures, which makes these habitats suitable for other species that are less adapted to disturbed environments. Also, seedlings can benefit from these shielded conditions. This has been shown by *Corenblit et al*. [2016] who find a positive feedback of older *P.nigra* on recruitment of *P.nigra* seedlings downstream of the vegetation patch.

Facilitation of native species by invaders seems rarer. Some case studies report native species facilitation by invaders due to changed habitat conditions such as the creation of refugia by reef building organisms or sea-grass [*Bially and MacIsaac*, 2000; *Castilla et al*., 2004; *Posey*, 1988]. In our model, we find facilitation due to the increased vegetation extent of both native and invading species creating larger vegetation patches and therefore more sheltered niches for Salicaceae species to survive. We only find this beneficial effect in the less persistent *F. japonica* scenarios when the native species are not completely out-competed by the invader (Table 6). In case of high propagule pressure, either with high or medium seed dispersal density, we do not find an increase in native vegetation spread or vegetated area. Only a combination of high *F. japonica* mortality and medium seed dispersal density decreases *F. japonica* spread, but Salicaceae species are not able to profit from these conditions (Figure 9). This suggests only a small "window" for native facilitation.

We only find facilitation when *F. japonica* acts as an additional eco-engineering species that actively modifies the environment thereby providing a positive feedback on settling native species. This is in line with the conceptual model of *Corenblit et al*. [2014] wherein *nondominant* alien species positively contribute to

the eco-engineering capacity of a system in enhanced trapping of sediment and facilitation of native species and alien species recruitment. This highlights that both invasive and native engineering plants are able to influence biogeomorphic succession.

In reality, invasion by *F. japonica* has several negative effects in addition to our modeled competition for space. It is known to have allelopathic abilities enabling the plant to excrete phytotoxic chemicals from its roots and hampering growth of Salicaceae species [*Dommanget et al*., 2014]. Furthermore, by changing vegetation structure and composition, other biota such as frogs, snails and mycorrhizal fungi might be affected [*Maerz et al*., 2005; *Stoll et al*., 2012; *Horackova et al*., 2015; *Zubek et al*., 2016]. This suggests that the facilitative effect of *F. japonica* in the model will most likely be overshadowed in reality by a range of other negative effects that could be included in future modeling. However, the facilitative effects in the less-resistant invader scenario could be valid for other alien plant species without additional negative effects on ecosystem functioning, but providing solely additional eco-engineering properties.

In this study, competition for space is a large contributor to invasion success. In reality a lot of other processes contribute to competition, which are not included in our model. For instance, *F. japonica* growth is hampered in grassland and areas with herbaceous vegetation. Including competition and interaction of these vegetation types would slow down the invasion of *F. japonica*, creating a more realistic areal expansion. All this raises the need for combined field surveys and modeling to identify the most important processes for large-scale effects. It has been shown that invaders can thrive in disturbed systems because of an altered resource balance that weakens native species and gives the invader competitive advantage [*Tickner et al*., 2001; *Huston*, 2004]. For instance, in case of hydrological alteration by dams, groundwater levels can drop and invasive species which are better able to adapt to this new situation by rapidly elongating their roots will gain an advantage [*Stromberg et al*., 2007b]. In natural systems where there is sufficient groundwater access, willow growth rates are correlated with moisture availability, while there is little correlation at locations where groundwater is less available [*Batz et al*., 2016]. Therefore, it will be more difficult for invaders to out-compete Salicaceae species in natural systems than in systems with altered flow regimes [*Merritt and Poff*, 2010].

The invasion speed of *F. japonica* in our study is relatively high because we assume unlimited rhizome transport in sediment and water. In reality, rhizomes are only transported downstream when morphodynamic activity has severed rhizomes from upstream *F. japonica* patches. Therefore, working with point-source populations of invasive plant propagules that will only be transported in case of morphodynamic activity, may generate more realistic vegetation patterns. Conversely, some effects of *F. japonica* might increase its expansion, for instance its allelopathic abilities or the influence of altered litter composition. Another effect that could increase local range expansion is the inclusion of lateral, vegetative growth, which may steadily increase its density over time, additional to the rhizome transport. Furthermore, to improve the predictive skills of the models, research should focus on unraveling vegetation response in terms of growth and succession related to hydro-morphodynamic pressures, such as erosion and sedimentation processes, altered groundwater access, flow velocities, flooding and desiccation in different types of systems and different life-stages of the vegetation. Other interesting research directions are to study how an invader could facilitate a secondary invasion [*Flory and Bauer*, 2014], to investigate the effect of river regulation on the spread of an invasive species [*Perkins et al*., 2015], or to investigate how other species inhabiting the floodplain are affected by the long-term interaction between invader, native vegetation and river morphodynamics. The coupled numerical model for hydro-morphodynamics and vegetation opens up many exciting new possibilities, discussed above, for investigating the effect of invasive species on the interaction with biota and landforms.

5.4. Seasonal Bio-morphodynamic Invasion Effects

The effect of an invader on river morphodynamics depends on the characteristics of the invader and those of the native plant species it is replacing. We considered a perennial invader that has an extensive belowground rhizome network, a high vegetation density in spring, summer and autumn, but dieback of aboveground biomass in winter. When this kind of invader replaces riparian species that maintain their biomass in winter, the substrate is more prone to erosion in winter resulting in higher sediment transport rates and faster river bank erosion (Figure 14d).

Indeed, it has been shown that *F. japonica* development increased soil erosion in late autumn and winter when vegetative growth died back, especially on steep river banks [*Child and Wade*, 2000]. This general

trend of increased river bank erosion in winter was also found for the highly invasive plant Himalayan Balsam (*Impatiens glandulifera*) [*Beerling and Perrins*, 1993; *Greenwood and Kuhn*, 2014; *Matthews et al*., 2015], which has similar seasonal above-ground dynamics as *F. japonica* but is less resistant to morphodynamic pressures. The main difference with *F. japonica* is that *I. glandulifera* is an annual plant, so that erosion in winter is likely even more intense because there is no active rooting system left for soil cohesion. In or model study however, we did neither take into account effects of the rooting system of *F. japonica* on soil strength, nor that dead stems remain erect during winter and thus can still provide some hydraulic resistance. Therefore, we most likely overestimate the amount of sediment transport over the floodplain in winter. River morphodynamics can be influenced by below-ground biomass, which is also shown by *Jaeger and Wohl* [2011], who studied the morphological response of the removal of two invasive species with and without removal of their rooting systems, and found that removal of all below-ground biomass caused significantly larger changes in channel adjustment. However, another field study shows that the root system of *F. japonica* provides far less stability on river banks in winter than forest and that the erosion rate of river banks vegetated with *F. japonica* approaches erosion rates of bare soil (D. Ross, personal communication, 2017). Clearly, more field data are needed including contextual information about the morphological style of the river.

Effects of vegetation are not merely local but also occur at reach-scale, because of the backwater effect on water levels. We find a large backwater effect in the high propagule pressure scenario in early autumn, when *F. japonica* is at its largest (Figure 14a). Hydraulic resistance values of *F. japonica*, indicated by stem density, are relatively high compared to those for most phases of Salicaceae (Figure 3b), which might increase the risk of flooding. In the high propagule pressure scenario, water levels are raised by almost 0.4 m on average in the growing season, when compared to winter. This is an extreme result because in the Allier River, discharges are generally higher in winter. In the other scenarios we do find higher water levels in winter compared to the growing season. In the low propagule pressure scenarios, the difference in water levels and sediment transport between seasons is least pronounced because there is a substantial vegetation cover in winter as well as in summer. Morphodynamic changes by invaders may be even more profound if an invasive species is an evergreen, perennial tree, such as *Tamarix*. This species is known to have caused changes in fluvial morphology by trapping sediment, increasing bank stability and narrowing the channel [*Tickner et al*., 2001]. Also invasive herbaceous vegetation can cause these effects by out-competing native species with a lower hydraulic roughness [*Martinez and McDowell*, 2016].

Our results show how seasonal vegetation properties and the interaction between vegetation and morphodynamic processes affect long-term river morphology. Modeling more aspects of bio-morphodynamics could lead to improved accuracy of results, e.g., by including native perennial, herbaceous vegetation interactions on the floodplain, including detailed relations between discharge, morphodynamics and above and below ground dynamics of Salicaceae species [*Pasquale et al*., 2014; *Tron et al*., 2015] and the inclusion of steep bank erosion processes that are currently not well represented by the coarse rectangular grid and the simple bank erosion algorithm [*Schuurman et al*., 2013]. Our modeling study provides generic working hypotheses to suggest data collection and test how invasive species in rivers and river morphodynamics interact in specific cases.

6. Conclusions

Our model results show that the effect of an invader on native riparian vegetation and river hydromorphodynamics is dependent on the magnitude of propagule pressure, its persistence, its dynamic properties and the dynamic properties of the native species it is replacing.

When propagule pressure is high, native species are out-competed due to fast and dense occupation of all available niches with a high persistence of the invader. Especially on higher elevations on the floodplain, where the invader is not removed by hydro-morphodynamic pressures, there is no room left for native species. This leads to a smaller range of native colonization at a lower floodplain elevation with higher morphodynamic pressures and consequently higher mortality rates. Additionally, dense invader vegetation patches concentrate the flow and create more hostile conditions around vegetation patches, creating a negative feedback that further limits native colonization.

When propagule pressure is smaller and the invader is less persistent, we find that native vegetation expands over a larger area. This is due to the development of larger, but less dense vegetation patches providing sheltered conditions that facilitate native colonization. In this case, the invader can be seen as an additional eco-engineering species contributing to the natural biogeomorphic succession in a similar way as the native vegetation. However, this positive effect is only visible when there is sufficient habitat available for native species, which was not the case in the high propagule pressure scenario. Also, additional negative effects, such as allelopathy by the invader would outbalance this facilitation effect.

When massive invasion of a perennial herbaceous species replaces riparian trees and leads to a dense vegetation cover, this may lead to considerable hydro-morphological effects. We observed an increase in water levels during the growing season in the scenarios with invaders, more so in the high propagule pressure scenario, creating a potential risk for flooding. Furthermore, we find a large difference in sediment transport rates between winter and autumn with relatively high erosion rates of the floodplains in winter when the above-ground biomass of the invader has died back. The scenario with the highest native abundance, facilitated by the invader, shows reduced erosion in winter due to the largest remaining above-ground biomass of the native species. This shows that seasonal above- and below ground dynamic vegetation properties of the invader and of the native vegetation it replaces will affect long-term morphological development of riparian areas.

Our work demonstrates that spatial and temporal patterns of local and large-scale effects of plant invasions are complicated because of the multiple bio-geomorphological feedback mechanisms. This exploratory model study led to new hypotheses for effects of invasive riparian species on fluvial biogeomorphology. Given the importance of the invasive species problem, spatiotemporal data of the invasive and native species in combination with data of river morphodynamics are urgently needed and will allow testing of our generalised conclusions.

Acknowledgments

We kindly thank Peter Horchler (Bundesanstalt für Gewässerkunde) for contributing to the setup of the *F. japonica* modeling, Peter Herman (Deltares) for reviewing the model code, Tom Buijse (Deltares) for reviewing and discussions to improve the manuscript and Barbara Grüner for *F. japonica* data and observations from the Schwechat River. We thank Carlo Camporeale and 4 anonymous reviewers for reviewing previous versions of the manuscript. This work was funded by REFORM (FP7 Grant Agreement 282656). The authors contributed in the following proportions to conception and design, model running, analysis and conclusions, and manuscript preparation: MvO (70%, 100%, 70%, 70%), MGK (10%, 0%, 15%, 10%), GG (5%, 0%, 5%, 5%), GE (10%, 0%, 2.5%, 2.5%), RL (5%, 0%, 2.5%, 2.5%), and HM (0%, 0%, 5%, 10%). Interested readers can request our data by contacting the corresponding author: mijke.vanoorschot@deltares.nl.

References

Aguilera, A. G., P. Alpert, J. S. Dukes, and R. Harrington (2010), Impacts of the invasive plant Fallopia japonica (Houtt.) on plant communities and ecosystem processes, *Biol. Invasions*, *12*(5), 1243–1252, doi:10.1007/s10530-009-9543-z.

Allstadt, A., T. Caraco, F. Molnár, and G. Korniss (2012), Interference competition and invasion: Spatial structure, novel weapons and resistance zones, *J. Theor. Biol.*, *306*, 46–60, doi:10.1016/j.jtbi.2012.04.017.

Baptist, M., V. Babovic, J. Rodriguez Uthurburu, R. Uittenbogaard, A. Mynett, and A. Verwey (2007), On inducing equations for vegetation resistance, *J. Hydraul. Res.*, *45*(4), 435–450, doi:10.1080/00221686.2009.9521996.

Batz, N., P. Colombini, P. Cherubini, and S. Lane (2016), Groundwater controls on biogeomorphic succession and river channel morphodynamics, *J. Geophys. Res. Earth Surf.*, *121*, 1763–1785, doi:10.1002/2014JF003432.

Beerling, D. J., and J. M. Perrins (1993), Impatiens glandulifera Royle (Impatiens roylei Walp.), *J. Ecol.*, *81*(2), 367–382, doi:10.2307/2261507.

Beerling, D. J., J. P. Bailey, and A. P. Conolly (1994), Fallopia japonica (Houtt.) Ronse Decraene, *J. Ecol.*, *82*, 959–979.

Berg, J. A., G. A. Meyer, and E. B. Young (2016), Propagule pressure and environmental conditions interact to determine establishment success of an invasive plant species, glossy buckthorn (Frangula alnus), across five different wetland habitat types, *Biol. Invasions*, *18*(5), 1363–1373, doi:10.1007/s10530-016-1073-x.

Bially, A., and H. J. MacIsaac (2000), Fouling mussels (Dreissena ssp.) colonize soft sediments in Lake Erie and facilitate benthic invertebrates, *Freshwater Biol.*, *43*, 85–97.

Bimova, K., B. Mandak, and I. Kasparova (2004), How does Reynoutria invasion fit the various theories of invasibility?, *J. Veg. Sci.*, *15*(4), 495–504, doi:10.1658/1100–9233(2004)015[0495:HDRIFT]2.0.CO;2.

Buckley, Y. M., D. T. Briese, and M. Rees (2003), Demography and management of the invasive plant species Hypericum perforatum, II. Construction and use of an individual-based model to predict population dynamics and the effects of management strategies, *J. Appl. Ecol.*, *40*(3), 494–507, doi:10.1046/j.1365-2664.2003.00822.x.

Castilla, J. C., N. A. Lagos, and M. Cerda (2004), Marine ecosystem engineering by the alien ascidian Pyura praeputialis on a mid-intertidal rocky shore, *Mar. Ecol. Prog. Ser.*, *268*, 119–130, doi:10.3354/meps268119.

Child, L., and M. Wade (2000), *The Japanese Knotweed Manual*, Packard Publishing Limited, Chichester, U. K.

Corenblit, D., E. Tabacchi, J. Steiger, and A. M. Gurnell (2007), Reciprocal interactions and adjustments between fluvial landforms and vegetation dynamics in river corridors: A review of complementary approaches, *Earth Sci. Rev.*, *84*(1–2), 56–86, doi:10.1016/j.earscirev.2007.05.004.

Corenblit, D., J. Steiger, and E. Tabacchi (2014), Ecosystem engineers modulate exotic invasions in riparian plant communities by modifying hydrogeomorphic connectivity, *River Res. Appl.*, *30*, 45–59, doi:10.1002/rra.

Corenblit, D., et al. (2016), Populus nigra establishment and fluvial landform construction: Biogeomorphic dynamics within a channelized river, *Earth Surf. Processes Landforms*, *41*(9), 1276–1292, doi:10.1002/esp.3954.

Dommanget, F., A. Evette, T. Spiegelberger, C. Gallet, M. Pacé, M. Imbert, and M. L. Navas (2014), Differential allelopathic effects of Japanese knotweed on willow and cottonwood cuttings used in riverbank restoration techniques, *J. Environ. Manage.*, *132*, 71–78, doi:10.1016/j.jenvman.2013.10.024.

Doody, T. M., P. L. Nagler, E. P. Glenn, G. W. Moore, K. Morino, K. R. Hultine, and R. G. Benyon (2011), Potential for water salvage by removal of non-native woody vegetation from dryland river systems, *Hydrol. Processes*, *25*(26), 4117–4131, doi:10.1002/hyp.8395.

EC (2014), Regulation (EU) No 1143/2014 of the European Parliament and of the Council of 22 October 2014 on the prevention and management of the introduction and spread of invasive alien species, *Off. J. Eur. Union*, *L317*, 35–55.

Eppinga, M. B., M. a. Kaproth, A. R. Collins, and J. Molofsky (2011), Litter feedbacks, evolutionary change and exotic plant invasion, *J. Ecol.*, *99*, 503–514, doi:10.1111/j.1365-2745.2010.01781.x.
Fei, S., J. Phillips, and M. Shouse (2014), Biogeomorphic impacts of invasive species, *Annu. Rev. Ecol. Evol. Syst.*, *45*, 69–87, doi:10.1146/annurev-ecolsys-120213-091928.
Flanagan, N. E., C. J. Richardson, and M. Ho (2015), Connecting differential responses of native and invasive riparian plants to climate change and environmental alteration, *Ecol. Appl.*, *25*(3), 753–767, doi:10.1890/14-0767.1.sm.
Flory, S. L., and J. T. Bauer (2014), Experimental evidence for indirect facilitation among invasive plants, *J. Ecol.*, *102*(1), 12–18, doi:10.1111/1365-2745.12186.
Geerling, G., A. Ragas, R. Leuven, J. van Den Berg, M. Breedveld, D. Liefhebber, and A. Smits (2006), Succession and rejuvenation in floodplains along the river Allier (France), *Hydrobiologia*, *565*(1), 71–86, doi:10.1007/s10750-005-1906-6.
Gerber, E., C. Krebs, C. Murrell, M. Moretti, R. Rocklin, and U. Schaffner (2008), Exotic invasive knotweeds (Fallopia spp.) negatively affect native plant and invertebrate assemblages in European riparian habitats, *Biol. Conserv.*, *141*(3), 646–654, doi:10.1016/j.biocon.2007.12.009.
Gillies, S., D. R. Clements, and J. Grenz (2016), Knotweed (Fallopia spp.) Invasion of North America utilizes hybridization, epigenetics, seed dispersal (Unexpectedly), and an arsenal of physiological tactics, *Invasive Plant Sci. Manage.*, *9*(1), 71–80, doi:10.1614/IPSM-D-15-00039.1.
Greenwood, P., and N. J. Kuhn (2014), Does the invasive plant, Impatiens glandulifera, promote soil erosion along the riparian zone? An investigation on a small watercourse in northwest Switzerland, *J. Soils Sediments*, *14*(3), 637–650, doi:10.1007/s11368-013-0825-9.
Grime, J. (2001), Colonisation and Invasion, in *Plant Strategies, Vegetation Patterns, and Ecosystem Properties*, 2nd ed., edited by J. Grime, chap. 7, pp. 225–237, John Wiley, Chichester, U. K.
Groeneveld, E., F. Belzile, and C. Lavoie (2014), Sexual reproduction of Japanese knotweed (Fallopia japonica s.l.) at its northern distribution limit: New evidence of the effect of climate warming on an invasive species, *Am. J. Bot.*, *101*(3), 459–466, doi:10.3732/ajb.1300386.
Gruener, B. (2016), Biologie,Oekologie und raeumlich-zeitliche Entwicklung des japanischen Staudenknoeterichs (Fallopia japonica): Eine Fallstudie an der niederoesterreichischen Schwechat, MSc thesis, Univ. of Nat. Resour. and Life Sci., Vienna.
Gurnell, A. (2014), Plants as river system engineers, *Earth Surf. Processes Landforms*, *39*(1), 4–25, doi:10.1002/esp.3397.
Habersack, H. M. (2000), The river-scaling concept (RSC): A basis for ecological assessments, *Hydrobiologia*, *422/423*, 49–60, doi:10.1023/A:1017068821781.
Hastings, A., et al. (2004), The spatial spread of invasions: New developments in theory and evidence, *Ecol. Lett.*, *8*(1), 91–101, doi:10.1111/j.1461-0248.2004.00687.x.
Hayen, B. (1995), Populationsökologische Untersuchungen an Reynoutria japonica [in German], in *Auswirkungen auf einheimische Arten, Lebensgemeinschaften und Biotope. Kontrollmöglichkeiten und Management*, edited by R. Bocker et al., pp. 125–140, Ecomed, Landsberg, Germany.
Horackova, J., S. Podrouzkova, and L. Jurickova (2015), River floodplains as habitat and bio-corridors for distribution of land snails: Their past and present, *J. Landscape Ecol.*, *8*(3), doi:10.1515/jlecol-2015-0012.
Horvitz, N., R. Wang, M. Zhu, F.-H. Wan, and R. Nathan (2014), A simple modeling approach to elucidate the main transport processes and predict invasive spread: River-mediated invasion of Ageratina adenophora in China, *Water Resour. Res.*, *50*, 9738–9747, doi:10.1002/2014WR015537.
Huston, M. A. (2004), Management strategies for plant invasions: Manipulating productivity, disturbance, and competition, *Diversity Distrib.*, *10*(3), 167–178, doi:10.1111/j.1366-9516.2004.00083.x.
Jaeger, K. L., and E. Wohl (2011), Channel response in a semiarid stream to removal of tamarisk and Russian olive, *Water Resour. Res.*, *47*, W02536, doi:10.1029/2009WR008741.
Kleinhans, M. G., and J. H. van den Berg (2011), River channel and bar patterns explained and predicted by an empirical and a physics-based method, *Earth Surf. Processes Landforms*, *36*, 721–738, doi:10.1002/esp.2090.
Lesser, G., J. Roelvink, J. van Kester, and G. Stelling (2004), Development and validation of a three-dimensional morphological model, *Coastal Eng.*, *51*, 883–915, doi:10.1016/j.coastaleng.2004.07.014.
Lockwood, J. L., P. Cassey, and T. Blackburn (2005), The role of propagule pressure in explaining species invasions, *Trends Ecol. Evol.*, *20*(5), 223–8, doi:10.1016/j.tree.2005.02.004.
Lowe S., M. Browne, S. Boudjelas, and M. De Poorter (2000), *100 of the World's Worst Invasive Alien Species A selection from the Global Invasive Species Database*, The Invasive Species Specialist Group (ISSG) a specialist group of the Species Survival Commission (SSC) of the World Conservation Union (IUCN), 12 pp.
Maerz, J. C., B. Blossey, and V. Nuzzo (2005), Green frogs show reduced foraging success in habitats invaded by Japanese knotweed, *Biodiversity Conserv.*, *14*(12), 2901–2911, doi:10.1007/s10531-004-0223-0.
Martinez, A. E., and P. F. McDowell (2016), Invasive Reed Canarygrass (Phalaris arundinacea) and native vegetation channel roughness, *Invasive Plant Sci. Manage.*, *9*(1), 12–21, doi:10.1614/IPSM-D-15-00046.1.
Matthews, J., R. Beringen, E. Boer, H. Duistermaat, B. Ode, J. Van Valkenburg, G. Van der Velde, and R. Leuven (2015), Risks and management of non-native Impatiens species in the Netherlands, technical report, Radbound Univ., FLORON, Naturalis Biodiversity Cent., Nijmegen, the Netherlands.
Merritt, D. M., and L. N. Poff (2010), Shifting dominance of riparian Populus and Tamarix along gradients of flow alteration in western North American rivers, *Ecol. Appl.*, *20*(1), 135–152, doi:10.1890/08-2251.1.
Odling-Smee, J., D. H. Erwin, E. P. Palkovacs, M. W. Feldman, and K. N. Laland (2013), Niche construction theory: A practical guide for ecologists, *Q. Rev. Biol.*, *88*(1), 4–28, doi:10.1086/669266.
Pasquale, N., P. Perona, R. Francis, and P. Burlando (2014), Above-ground and below-ground Salix dynamics in response to river processes, *Hydrol. Processes*, *28*(20), 5189–5203, doi:10.1002/hyp.9993.
Perkins, D., M. Scott, and T. Naumann (2015), Abundance of invasive, non-native riparian herbs in relation to river regulation, *River Res. Appl.*, *24*(7), 941–959, doi:10.1002/rra.
Peterson, A. T., and D. A. Vieglais (2001), Predicting species invasions using ecological Niche Modeling: New approaches from bioinformatics attack a pressing problem, *BioScience*, *51*(5), 363–371, doi:10.1641/0006–3568(2001)051[0363:PSIUEN]2.0.CO;2.
Posey, M. H. (1988), Community changes associated with the spread of an introduced seagrass, Zostera japonica, *Ecology*, *69*(4), 974–983, doi:10.2307/1941252.
Richardson, D. M., P. M. Holmes, K. J. Esler, S. M. Galatowitsch, J. C. Stromberg, S. P. Kirkman, P. Pysek, and R. J. Hobbs (2007), Riparian vegetation: Degradation, alien plant invasions, and restoration prospects, *Diversity Distrib.*, *13*, 126–139, doi:10.1111/j.1472-4642.2006.00314.x.
Rodriguez, L. F. (2006), Can invasive species facilitate native species? Evidence of how, when, and why these impacts occur, *Biol. Invasions*, *8*(4), 927–939, doi:10.1007/s10530-005-5103-3.

Santoro, R., T. Jucker, M. Carboni, and A. T. Acosta (2012), Patterns of plant community assembly in invaded and non-invaded communities along a natural environmental gradient, *J. Veg. Sci.*, *23*(3), 483–494, doi:10.1111/j.1654-1103.2011.01372.x.

Schuurman, F., W. A. Marra, and M. G. Kleinhans (2013), Physics-based modeling of large braided sand-bed rivers: Bar pattern formation, dynamics, and sensitivity, *J. Geophys. Res. Earth Surf.*, *118*, 2509–2527, doi:10.1002/2013JF002896.

Shaw, R. H., R. Tanner, D. Djeddour, and G. Cortat (2011), Classical biological control of Fallopia japonica in the United Kingdom - lessons for Europe, *Weed Res.*, *51*(6), 552–558, doi:10.1111/j.1365-3180.2011.00880.x.

Shimoda, M., and N. Yamasaki (2016), Fallopia japonica (Japanese Knotweed) in Japan: Why is it not a pest for Japanese people?, in *Vegetation Structure and Function at Multiple Spatial, Temporal and Conceptual Scales*, edited by E. O. Box, chap. Part V, pp. 447–473, Springer Int. Publ., Switzerland, doi:10.1007/978-3-319-21452-8.

Simberloff, D. (2013), *Invasive Species. What Everyone Needs to Know*, Oxford Univ. Press, New York.

Solari, L., M. Van Oorschot, B. Belletti, D. Hendriks, M. Rinaldi, and A. Vargas-Luna (2016), Advances on modelling riparian vegetation-hydromorphology interactions, *River Res. Appl.*, *32*, 164–178, doi:10.1002/rra.2910.

Stoll, P., K. Gatzsch, H. P. Rusterholz, and B. Baur (2012), Response of plant and gastropod species to knotweed invasion, *Basic Appl. Ecol.*, *13*(3), 232–240, doi:10.1016/j.baae.2012.03.004.

Stromberg, J. C., S. J. Lite, R. Marler, C. Paradzick, P. B. Shafroth, D. Shorrock, J. M. White, and M. S. White (2007a), Altered stream-flow regimes and invasive plant species: The Tamarix case, *Global Ecol. Biogeogr.*, *16*(3), 381–393, doi:10.1111/j.1466-8238.2007.00297.x.

Stromberg, J. C., V. B. Beauchamp, M. D. Dixon, S. J. Lite, and C. Paradzick (2007b), Importance of low-flow and high-flow characteristics to restoration of riparian vegetation along rivers in arid south-western United States, *Freshwater Biol.*, *52*, 651–679, doi:10.1111/j.1365-2427.2006.01713.x.

Temmerman, S., T. Bouma, J. Van de Koppel, D. Van der Wal, M. De Vries, and P. Herman (2007), Vegetation causes channel erosion in a tidal landscape, *Geology*, *35*(7), 631, doi:10.1130/G23502A.1.

Thomson, D. M. (2005), Matrix Models as a tool for understanding invasive plant and native plant interactions, *Conserv. Biol.*, *19*(3), 917–928, doi:10.1111/j.1523-1739.2005.004108.x.

Tickner, D. P., P. G. Angold, a. M. Gurnell, and J. O. Mountford (2001), Riparian plant invasions: Hydrogeomorphological control and ecological impacts, *Prog. Phys. Geogr.*, *25*(1), 22–52, doi:10.1177/030913330102500102.

Tron, S., P. Perona, L. Gorla, M. Schwarz, F. Laio, and L. Ridolfi (2015), The signature of randomness in riparian plant root distributions, *Geophys.l Res. Lett.*, *42*, 7098–7106, doi:10.1002/2015GL064857.

Urgenson, L. S., S. H. Reichard, and C. B. Halpern (2014), Habitat Factors and Species' Traits Influence Riparian Community Recovery Following Removal of Bohemian Knotweed (Polygonum x bohemicum), *BioOne*, *88*(3), 246–260, doi:10.3955/046.088.0307.

Van Dijk, W. M., F. Schuurman, W. I. Van de Lageweg, and M. G. Kleinhans (2014), Bifurcation instability and chute cutoff development in meandering gravel-bed rivers, *Geomorphology*, *213*, 277–291, doi:10.1016/j.geomorph.2014.01.018.

van Oorschot, M., M. Kleinhans, G. Geerling, and H. Middelkoop (2016), Distinct patterns of interaction between vegetation and morphodynamics, *Earth Surf. Processes Landforms*, *41*, 791–808, doi:10.1002/esp.3864.

Vollmer, I. (2012), Wiederholungsuntersuchen zur Besiedlung der invasiven Neophyten [in German], tech. report, BfG, Koblenz.

Weston, L. A., J. N. Barney, and A. DiTommaso (2005), A Review of the biology and ecology of three invasive perennials in New York State: Japanese Knotweed (Polygonum cuspidatum), Mugwort (Artemisia vulgaris) and Pale Swallow-wort (Vincetoxicum rossicum), *Plant Soil*, *277*(1–2), 53–69, doi:10.1007/s11104-005-3102-x.

Xiao, S., R. M. Callaway, G. Newcombe, and E. T. Aschehoug (2012), Models of experimental competitive intensities predict home and away differences in invasive impact and the effects of an endophytic mutualist, *Am. Nat.*, *180*(6), 707–18, doi:10.1086/668008.

Zubek, S., M. L. Majewska, J. Błaszkowski, A. M. Stefanowicz, M. Nobis, and P. Kapusta (2016), Invasive plants affect arbuscular mycorrhizal fungi abundance and species richness as well as the performance of native plants grown in invaded soils, *Biol. Fertil. Soils*, *52*(6), 879–893, doi:10.1007/s00374-016-1127-3.